GROWTH OF MAGNETRON SPUTTERED SUPERCONDUCTOR MgB_2 THIN FILMS

A Thesis Submitted to
the Graduate School of Engineering and Science of
İzmir Institute of Technology
in Partial Fulfillment of the Requirements for the Degree of

MASTER OF SCIENCE

in Physics

by
Savaş ULUCAN

July 2006
İZMİR

We approve the thesis of **Savaş ULUCAN**

Date of Signature

…… **20 July 2006**
Assoc. Professor Lütfi ÖZYÜZER
Supervisor
Department of Physics
İzmir Institute of Technology

…… **20 July 2006**
Assoc. Professor Salih OKUR
Department of Physics
İzmir Institute of Technology

…… **20 July 2006**
Professor Doğan ABUKAY
Department of Physics
İzmir Institute of Technology

…… **20 July 2006**
Professor Hüseyin Zafer DURUSOY
Department of Physics Engineering
Hacettepe University

…… **20 July 2006**
Professor Mustafa EROL
Department of Physics Education
Dokuz Eylül University

…… **20 July 2006**
Prof. Durmuş Ali DEMİR
Head of Department
İzmir Institute of Technology

……
Assoc. Prof. Dr. Semahat ÖZDEMİR
Head of the Graduate School

ACKNOWLEDGMENTS

I would like to thank my thesis advisor Asst. Professor Lütfi Özyüzer for his guidance, continuous support and encouragement throughout the preparation of this thesis.

I am greatly indebted to the staff of Center for Material Research of İzmir Institute of Technology for their contribution. During this graduate study, I acknowledge the financial support from TUBITAK and DPT. I wish to extend my thanks to İzmir Institute of Technology for providing Research Assistantship during my thesis.

I would like to express my gratefulness to Professor Selçuk Atalay for their contribution to this thesis with providing the opportunity for electrical measurements at İnönü University.

I am also thankful to my colleagues, Kaan Oğuz, Kadir Vahaplar, Yılmaz Şimşek and Mehtap Özdemir for their helpful discussion.

Finally, special thanks to my best friends Mert Atacan, Emre Öznehir, my brother Ozan Ulucan and my family for their support and motivation.

ABSTRACT

GROWTH OF MAGNETRON SPUTTERED SUPERCONDUCTOR MgB_2 THIN FILMS

The discovery of superconductivity in the intermetalic compound MgB_2 (39 K) in 2001 raised the great interest for the both science and technology applications. It has the highest T_c value among the intermetalic compounds. MgB_2 has many properties make it very attractive for superconducting applications; these are large coherence length, high critical current density (J_c), high critical magnetic field (B_c) values. There are several methods developed to produce high quality MgB_2 superconducting thin films. Magnetron sputtering system is a widely used method to deposit thin films. In this study, an MgB_2/Mg target was produced by using MgB_2 and Mg powders with a hot press technique. Prepared sputtering target used to grow MgB_2 superconducting thin films on Al_2O_3 polycrystal and $LaAlO_3$ single crystal substrate by a high vacuum magnetron sputtering system. To enhance the superconducting properties of as-grown films and to increase the crystal quality of the as-grown film an ex-situ anneal process was examined. X-Ray Diffraction (XRD) method was used to obtain crystal structure of the grown films. To observe the surface morphology of the films and to measure the thickness of the films Scanning Electron Microscopy (SEM) images were taken. Electron Dispersive X-Ray Spectroscopy (EDX) technique was used to identify the chemical contents of the films. Low temperature electrical measurement was done under various magnetic fields to observe the superconducting behavior of prepared films. The effects of ex-situ annealing process were also investigated. It was found that ex-situ annealing process develops the structural and electrical properties of MgB_2 thin films.

ÖZET

MIKNATISSAL PÜSKÜRTME İLE ÜSTÜN İLETKEN MgB_2 İNCE FİLMLERİN BÜYÜTÜLMESİ

2001 yılında, intermetalik bir bileşik olan MgB_2' deki (39 K) üstün iletkenlik özelliğinin keşfi hem bilimsel hemde teknolojik uygulamalardaki ilgiyi arttırdı. MgB_2, intermetalik bileşikler arasında en yüksek geçiş sıcaklığına sahip malzemedir. MgB_2' ın sahip olduğu özellikler, bunlar; uzun koharens uzunluğu, yüksek kritik akim yoğunluğu değeri (J_c) ve yüksek kritik manyetik alan değeridir (B_c), onu üstün iletkenlik uygulmaları için çok çekici bir hale getirmiştir. Yüksek kalitede MgB_2 üstün iletken film üretmek için geliştirilmiş bir çok yöntem bulunmaktadır. Mıknatıssal püskürtme sistemi, film üretmek için çok kullanlıan bir yöntemdir. Bu çalışmada, sıcak sıkıştırma yöntemi ile MgB_2 ve Mg tozlar kullanılarak bir adet MgB_2/Mg püskürtme hedefi üretilmiştir. Hazırlanan hedef, yüksek vakum mıknatıssal püskürtme sistemi ile Al_2O_3 poli kristal alttaş ve $LaAlO_3$ tek kristal alttaş üzerine MgB_2 üstün iletken ince film büyütmek için kullanılmıştır. Ek işlemsiz büyütülmüş filmlerin üstüniletkenlik özelliklerinin iyileştirilmesi ve kristal yapısının yükseltilmesi için, film büyütme sisteminden farklı bir ortamda gerçekleştirilen ısıl işlem uygulanmıştır. Büyütülen filmlerin kristal yapısını tanımlamak için X ışınları difraksiyon (XRD) yöntemi kullanılmıştır. Filmlerin yüzey morfolojisini incelemek ve filmlerin kalınlıklarını ölçmek için taramalı electron mikroskop (SEM) görüntüleri alındı. Filmlerin kimyasal içeriğini tayin etmek için elekton ayırıcı X ışınları spektroskopisi (EDX) yöntemi kullanılmıştır. Hazırlanan filmlerin üstün iletkenlik özelliklerinin gözlenmesi için farklı manyetik alanlar altınd düşük sıcaklıklarda elektriksel ölçümler yapıldı. Film büyütme sisteminden farklı bir ortamda gerçekleştirilen ısıl işlemin etkileri incelendi. Gerçekleştirilen ısıl işlemin MgB_2 ince filmlerin yapısal ve elektriksel özelliklerini geliştirdiği bulunmuştur.

TABLE OF CONTENTS

LIST OF FIGURES

LIST OF TABLES

CHAPTER 1

INTRODUCTION

Superconductivity, a very interesting phenomenon, marked a great interest in solid state physics. After discovery of superconductivity, many researches tried to explain this phenomenon both in theoretical and in experimental ways. After these efforts, many materials were found showing superconductor behavior at high temperatures above 77 K, the boiling point of liquid Nitrogen. These materials have various application areas in technology. The thin film growth of MgB_2 is necessary for electronic applications. Recent discovery of MgB_2 (39 K), as an intermetallic compound, is very important for energy and electronic applications of thin film technology.

1.1. History of Superconductivity

The superconductivity was first observed in Mercury by Dutch physicist Heike Kamerlingh Onnes of Leiden University in 1911. He found that the electrical resistivity of Mercury suddenly undergoes to an immeasurably small value at a temperature of nearly 4.2 K (Onnes 1911). The next important milestone in superconductivity is perfect diamagnetism observed in 1933 by two German scientists, W. Meissner and R. Ochnefeld. They founded that the magnetic field is expelled by the superconductor below a certain temperature, T_c (Meissner and Ochsenfeld 1933). The first widely-accepted theoretical understanding of superconductivity was suggested in 1957 by American physicists John Bardeen, Leon Cooper, and John Schrieffer. Their theory of superconductivity became know as the BCS theory - derived from the first letter of each man's last name - and won them the Nobel Prize in 1972. The mathematically-complex BCS theory explained superconductivity at temperatures close to absolute zero for elements and simple alloys (Barden et al. 1957). However, at higher temperatures and with different superconductor systems, the BCS theory has subsequently become deficient to fully explain how superconductivity is occurring.

After discovery of superconductivity at Mercury by Onnes, several new materials showing superconductor behavior was found that have higher transition

temperature, T_c, with ongoing researches. In 1987, Yttrium Barium Copper Oxide ($YBa_2Cu_3O_7$) was found with a 93 K transition temperature that is above the boiling temperature of liquid nitrogen (77K). This was an important breaking point because of higher cost of the liquid He (10 $/lt) than that of the liquid Nitrogen (1 $/lt). The highest critical temperature is above 130 K in HgBaCaCuO. These superconductors are called high temperature superconductors.

In 2001, a Japanese researcher, Akimitsu, and his colleges discovered superconductivity in MgB_2 with a 39 K transition temperature (Nagamatsu et al. 2001). This temperature was a record for a simple inter metallic compound, because the highest transition temperature of a metallic compound was 23.4 K in Nb_3Ge (Gaveler et al. 1974) before discovery of superconducting property of MgB_2. After discovery of superconductivity in MgB_2, many investigations were performed to explain theoretical and experimental background of its superconducting properties. The superconducting application for cables made of MgB_2 is an important efficient energy system. On the other hand, MgB_2 thin film production techniques were developed for electronic applications.

1.2. Fundamental Properties of Superconductivity

In all metals, if the temperature is lowered, the resistances of the metals become smaller and smaller at a constant rate. On the other hand, the main property of superconductivity is zero resistance below a certain critical temperature. This temperature is defined transition temperature, T_c. When the superconductor material is cooled, the resistivity of the superconductor material drops suddenly to near zero value at a transition temperature. This is first observed by Onnes at Mercury (4.2 K) in 1911.

Another main property of the superconductivity is perfect diamagnetism. The magnetic properties of superconductor materials are equally important like zero resistance for technological applications. This phenomenon is known as Messiner and Oshchenfeld effect. If a superconductor is cooled below transition temperature under magnetic field, it will exclude the magnetic field lines throughout the materials. Below a transition temperature, the net magnetic field in the superconductor equals to zero (B=0). But superconductivity disappears at the critical applied magnetic field, B_c. This critical magnetic field value is a characteristic of the material. Meissner and

Oshchenfeld effect is very important for superconductivity in technological applications for example MAGLEVs.

All superconductors can be described by their magnetic properties. They are classified in two groups with respect to their magnetic behavior, type I and type II. In type I superconductors, the whole material completely transforms from normal state to superconductor state at a critical transition temperature and critical magnetic field value. In the type II class, this transition occurs partially between lower and upper critical magnetic field. This region between upper and lower magnetic field is called mixed state. In the mixed state both superconductor and normal state is observed. While type I materials are elements but type II materials are generally compounds.

Another important characteristic feature of the superconducting state is that, superconductivity vanishes when the current density through the sample exceeds a critical value, critical current density (J_c). This is not an astonishing situation because the current through the superconductor will itself generate a magnetic field and at sufficiently high current densities, the magnetic field at the surface of the specimen will exceed the critical field and superconductivity disappears. However, this direct relation between critical field (B_c) and critical current density (J_c) is only true for type II superconductors.

1.3. Superconducting Thin Films and Applications

Superconducting materials are used in several industrial applications. Recently, superconducting thin films are the most popular application for electronic industry. Development of technology increased the interest of thin film technology. Most of the applications are based on superconducting thin film technology rather than wires, since the total currents are needed are not so large. Superconductors exhibit extremely small resistance at radio frequency (RF) and microwave frequencies and resonance cavities, lossless transmission structures, and application relies on the transition between the superconducting and the normal state. In an ideal superconductor, the resistivity transition at T_c is very sharp, that appears the basis for variety of thermally based detectors and switches. That means, a superconductor held a T_c can be very sensitive Bolometer or thermal detector for heat radiation.

Superconductor thin films are used in electronic devices such as the Josephson junctions have provided the basis for the widest range of superconducting electronic devices. Superconducting Quantum Interference Device (SQUID) magnetometers are the most sensitive detectors of low frequency magnetic fields, available in any technology.

Since the discovery of the first high temperature superconductor (HTS) (Bednorz and Muller 1986), a significant effort has been put into the research on epitaxial HTS films. There are several techniques to deposit HTS materials; sputtering techniques, Moleculer Beam Epitaxy (MBE) systems, Pulsed Laser Deposition (PLD) etc. These techniques are described in topical review by Wördenweber (Wördenweber 1999). Unfortunately, anisotropic and ceramic natures of HTS as well as small coherence length make them difficult as a junction for electronic applications.

Considered a main point in superconductivity, discovery of superconductivity in MgB_2 is very important for fabricating junctions because of MgB_2 superconducting properties. Its critical temperature of 39 K enables electronic device based on MgB_2 to operate at 20-25 K or even 30 K, which gives a significant advantage to this material compared to low temperature superconductors like Nb. Nb-based superconducting integrated circuits must operate at temperatures close to 4.2 K that requires heavy cyrocoolers with a large amount of power and is not acceptable for most electronic applications. Circuits based on HTS would solve this problem; reproducible HTS Josephson junctions with sufficiently small variations in device parameters have not been produced. An MgB_2-based circuit operates at 25 K that is a good solution for these problems. (Zeng et al. 2002).

MgB_2 is simpler, cheaper and more stable over time compared to HTS, making it attractive for a number of applications. For example, in the case of SQUID based on MgB_2 less noise is expected, giving a certain advantage for electronic circuits made in MgB_2 (Mijatovic et al. 2005). It was noticed that in the case of dc-SQUIDs, the low frequency noise and is 2-3 orders of magnitude lower than that of YBCO SQUIDs early in their development (Zhang et al. 2001). These results are very encouraging for the development of superconducting electronics and devices operating at 20-30 K based on MgB_2. It was found that MgB_2 is capable of transporting high critical currents, unlike the HTS. Increasing in the critical current density value made this material for electronic applications.

1.4. Objective of Thesis

MgB_2 is a significant material on the superconductivity field for a number of reasons. As mentioned, its high critical temperature, high critical magnetic field and high current densities make it very suitable for energy applications. The intensive studies on MgB_2 growth of thin films make technology future for industry. There are several thin film applications to improve the properties of superconductor devices. MgB_2 suggests a higher operating temperature (20 K) than the current technology in use by Nb based superconductors.

High quality MgB_2 thin films are necessary for MgB_2 Josephson junctions. Several methods were examined to deposit MgB_2 thin film because of growth difficulties of MgB_2. High vapor pressure of Mg and its sensitivity to oxidation are main problems of growth techniques. To overcome these problems ex-situ and in-situ methods were used. Generally, Pulsed laser deposition (PLD) (Brinkman et al. 2001), Molecular Beam Epitaxy (MBE) (Ueda and Naito 2002), various evaporation methods (Zeng et al. 2003, Monticone et al. 2004) were used to perform high quality MgB_2 thin films with high critical temperature, high critical magnetic field and critical current density.

In addition to these growth methods, sputtering method is widely used in deposition MgB_2 thin films. Magnetron sputtering system has some advantage for growth of thin films. Firstly magnetron sputtering systems are more economical than other complex techniques, like MBE, PLD. In addition to this, it has high deposition rate according to conditions. Then, magnetron sputtering systems are very suitable for large area thin film growth. These advantages make the magnetron sputtering system an important tool to deposit MgB_2 thin film production.

In this study, our aim is to grow superconducting MgB_2 thin films by a magnetron sputtering system. Firstly, we prepared a MgB_2 target for the magnetron sputtering system to deposit thin films. Commercially MgB_2 (purity 98.5%) and Mg (purity 99.99%) powder were used to perform a suitable sputtering target for the system by using a hot press techniques. MgB_2 thin films were grown on Al_2O_3 polycrystal substrate and $LaAlO_3$ single crystal substrate with an orientation (001). After deposition of thin films, we performed an ex-situ process to increase the crystal quality of the films and to enhance the superconducting properties of the films. In ex-situ process, we tried

to investigate the post-annealing conditions for as-grown films. Low temperature electrical properties of the films, 10 K- 300 K, were performed to show superconducting properties under different magnetic fields. To demonstrate the crystal structure of the films, X-Ray diffraction (XRD) method was used. In addition to this structure characterization, scanning electron microscopy (SEM) technique for microstructure and surface morphology and Energy dispersive X-Ray (EDX) technique for chemical contents of the films were examined.

In the next chapter, we will explain structural and superconducting properties, MgB_2 thin film deposition techniques, and growth parameters. Then, we will present our experimental procedure used for production of MgB_2 thin films and characterization techniques will be given in chapter 3. Chapter 4 includes our results and discussions about characterization results of the prepared films. At the end of this thesis, we will conclude our results.

CHAPTER 2

MgB_2 AND THIN FILMS

2.1. MgB_2

2.1.1. Crystal Structure of MgB_2

MgB_2 is not a new material; it is synthesized in the middle of the 1950's. However, superconducting properties of this material were discovered by Akimitsu in 2001 (Nagamatsu et al. 2001). MgB_2 is an inter-metallic compound. It has the highest transition temperature, 39 K, among the known metallic compound materials. It consists of Mg and B atoms. It has very simple crystal structure.

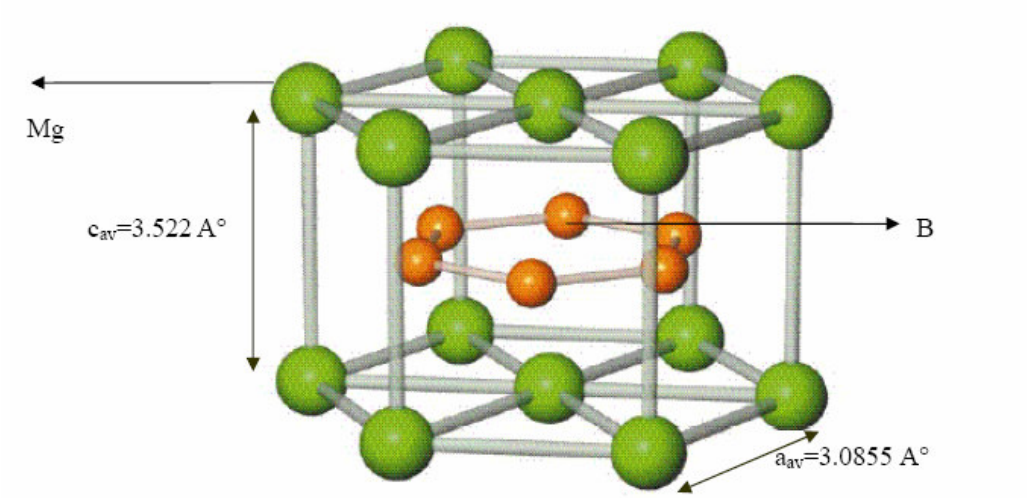

Figure 2.1. The crystal structure of MgB_2

(Source: Larbalestier et al. 2001)

MgB_2 crystal structure can be defined that of simple hexagonal AlB2-Type materials. Figure 2.1 represents the schematic of the MgB_2 crystal structure (Larbalestier et al. 2001). The structure consists of hexagonal-closed packed (hcp) layers of Mg atoms and graphite-like honeycomb layers of B atoms. At room temperature, lattice parameters of hexagonal MgB_2 are a=3.0885 A° and c= 3.522 A°.

These are the main characteristics of simple MgB_2 structure of which properties, crystal structure and lattice parameters, are very important parameters for deposition of MgB_2 thin films because the substrate has to be match crystal structure of MgB_2.

2.1.2. Superconductivity of MgB_2

2.1.2.1. Superconductivity Mechanism of MgB_2

Most of the fundamental superconducting properties of MgB_2 were explained by many groups. Here, we will give a brief description for these properties of MgB_2. It has ~39 K transition temperature. To explain this high critical temperature, it is crucial to know superconductivity mechanism in MgB_2. MgB_2 appears to be a phonon-mediated BCS superconductor. It was showed by the isotope effect. The isotope effect is one of the fundamental tests for superconductivity mechanism. In a conventional BCS superconductor, where cooper paring is mediated by phonons, the isotope effect exponent (α in $T_c \sim M^{-\alpha}$) is 0.5. The isotope effect for MgB_2 is first measured by Bud'ko (Bud'ko et al. 2001) and Hinks (Hinks et al. 2001). B and Mg are light elements. The boron isotope exponent, 0.26-0.30, is bigger than that of Mg, 0.02. A large boron isotope effect was reported, based on observation of the temperature dependent magnetization, resistance and specific heat on $Mg^{10}B_2$ and $Mg^{11}B_2$ samples. One Kelvin shift of transition temperature was observed in these experiments. The results strongly support phonon-mediated superconductivity in MgB_2 with B atom vibrations substantially involved and it is proved that Mg has a small effect in T_c of MgB_2. The total isotope exponent, for a multi component system, the isotope effect can be defined by the sum of the isotope exponent of all components, ($\alpha_t = \alpha_{Mg} + \alpha_B$), is close to 0.32, lower than the ideal value of 0.5. It can be explained by either strong coloumb repulsion or by large anharmonicity of B atom vibrations. Moreover, to explain why its transition temperature is so high, two independent studies were published in the summer of 2001 (Osborn et al. 2001, Yıldırım et al. 2001). They have obtained the phonon density of states of MgB_2 by experimentally from the neutron scattering measurements on polycrystalline samples to calculate the transition temperature of MgB_2. Results of these studies confirm that a conventional phonon mechanism, with moderately strong electron-phonon coupling, can explain the observed superconductivity in MgB_2.

In addition to this, the energy gap plays an important role in BCS theory. Thus, studying and calculating energy gaps can help to explain mechanism of superconductivity in this compound. MgB_2 is an example for a two band gap superconductor material. In order to find the superconducting energy gaps (Δ), a lot of techniques were performed, those were point contact spectroscopy (Schmidt et al. 2001), specific heat measurements (Bouquet et al. 2001), and scanning tunneling spectroscopy (Iavarone et al. 2002,). According to these literatures, two energy gaps were found at Δ= 1.8 mV and 7.5 mV.

2.1.2.2. Superconducting Properties of MgB_2

As mentioned in previous sections, MgB_2 has the highest critical temperature, 39 K, among the inter-metallic compounds. It has an advantage for industrial applications that has operating points above 20 K. The resistivity of MgB_2 at room temperature 5-6 $\mu\Omega$ cm, which can be compared to ρ (300 K) of ~2 $\mu\Omega$.cm for Cu, ~15 $\mu\Omega$.cm for Nb, ~80 $\mu\Omega$.cm for Nb_3Sn, and 100-150 $\mu\Omega$.cm for YBCO. However the low temperature resistivity still differs group to group: 0.3-3 $\mu\Omega$.cm in bulk form or thin film form (Rowell 2003).

Moreover, another main property of superconductor materials is diamagnetism. MgB_2 is Type II superconductor, according to its magnetic properties. The upper critical field of MgB_2 is anisotropic because of its layered structure. Recent measurements show that H_{c2} parallel to c axis is about 3 to 4 T at T=0 K and H_{c2} value parallel to ab axis about 15-20 T at T=0 K. The calculated anisotropy is ~4 from these results (Buzea and Yamashita 2001). The highest values of the upper critical field are achieved for thin films, $H_{c2}(0)$ =32 T, (Jung et al. 2001). The second best values for the upper critical are attained by single crystals, $H_{c2}(0)$ =25 T, (Xu et al. 2001), followed by bulk with $H_{c2}(0)$ =19 T. The lower critical field H_{c1} is also anisotropic. The value of the lower field, H_{c1}, is 27.2 mT along the c axis and 38.4 mT along the ab axis at T= 0 K in a single crystal (Xu et al. 2001). In addition to this, the calculated values of Ginzburg-Landau (GL) coherence length of the MgB_2 is ξ_{ab}= 5-8 nm and ξ_c= 2-3 nm.

Many groups have measured the critical current density and its temperature and magnetic field dependence for different forms of MgB_2; powders, bulk, films, tapes and wire. Kim et al reported the critical current densities (J_c) in MgB_2 thin film values of 4.0

x 10^6 A.cm^{-2} at 5 K and 0 T, 0.1 x 10^6 A.cm^{-2} at 15 K and 5 T (Kim et al. 2001). To take advantage of the relatively high T_c of 39 K of MgB_2, it is important to have high J_c values at temperatures above 20 K. The boiling point of H at atmospheric pressure is 20.13 K, so it is possible to use liquid hydrogen as a cryogen for cooling MgB_2.

2.2. Thin Films and Growth Kinetics

In recent years, thin film science has grown world-wide into a major research area. The importance of coatings and the synthesis of new materials for industry have resulted in a tremendous increase of innovative thin film processing technologies.

Thin film growth has some growth modes. Many observations of subsequent film formation have pointed to three basic growth modes: (1) *island (or Volmer-weber)*, (2) *layer (Frank-Van der merwe)* and (3) *Stranski-Krastonov* (Ohring 2002). Island growth occurs when the smallest stable clusters nucleate on the substrate and grow in three dimensions to form islands. This happens when atoms or molecules in the deposit are most strongly bound to each other than to the substrate. The opposite characteristics are displayed during the layer growth. Here the extensions of the smallest nucleus occur in two dimensions resulting in the formation of planar sheets. In this growth mode the atoms are more strongly bound to the substrate than to each other. The first complete monolayer is then covered with somewhat less tightly bound second layer. The layer plus island or Stranski-Krastonov growth mechanism is an intermediate combination of the proceeding two modes. In this case after forming one or more monolayer, one subsequent layer growth becomes unfavorable and island forms.

Some conditions are necessary for thin film growth. These are substrate choice, deposition temperature, surface energies and deposition pressure according to growth methods. Firstly, substrate choice is very important step for formation of thin films. In this case lattice parameters perform very important role. Films can be grown in amorphous crystal structure, polycrystal or single crystal structure. This is related to substrate lattice parameters and film material lattice parameters. Generally, an important quantity is the lattice misfit, f,

$$f= [a_0(s) - a_0(f)] / a_0(f) \qquad (2.1)$$

can be described as in equation 2.1 (Ohring 2002). Here, $a_o(f)$ and $a_o(s)$ refer to the lattice parameters of film and substrate. Desirable structure of the thin films, suitable substrate should be chosen. Secondly, growth kinetics of the thin films is settled down on the thermodynamics of the grown films and substrate. In this case; the phase diagrams of the growth material is very important parameter to grow of good quality thin films. To deposit the better quality thin films, substrate can be heated. This deposition temperature can be founded by phase diagram of the growth materials. In addition to this step, surface and film interactions can be thought to be another important parameter. Substrate should not react with the deposited film in deposition temperature. Finally, according to growth methods, the deposition pressure should be adjusted from the phase diagram of the film material. These are some fundamentals of the good quality thin film growth.

Advancing the technology of thin film science, several growth techniques were developed. Generally, two main growth methods are examined, which are chemical vapor deposition (CVD) and physical vapor deposition (PVD). These two main growth techniques can be separated in a few categories including evaporation methods, glow discharge methods, gas-phase chemical process and liquid-phase chemical techniques.

2.3. Sputtering Process

Sputtering in its many forms has become perhaps the most widespread used physical vapor deposition process. When a solid surface is bombarded with energetic particles such as accelerated ions, surface atoms of the solids are scattered backward due to the collisions between the surface atoms and the energetic particles. This phenomenon is called sputtering. Since the sputtering is the process of ejection of the surface atoms by the collisions between energetic ions, sputter deposition is nothing more than the accumulation of these ejected particles onto a nearby surface. This phenomenon is used widely in a number of areas such as, film deposition on semiconductor wafers, magnetic media and head surfaces, reflective coatings on glass and a number of other wide ranging applications.

Sputtering is usually practiced by means of plasmas which generate charged particles that can be accelerated towards a surface electrically. The term “glow discharge” refers to the light given of by plasma. Plasma is a partially ionized gas.

Figure 2.2 shows the simple plasma reactor. Two parallel plates are contained in a vacuum system and attached to a dc power supply. In such a dc glow discharge process, if the voltage is high enough, the field in the reactor will exceed the breakdown field of the gas, and a high voltage arc will flash between two electrodes. This arc will create a large number of ions and free electrons. Because of the electric field in the chamber, the electrons will be accelerated toward the positively charged anode, and the ions will be accelerated toward the negatively charged cathode. Due to their small mass, the electrons will be accelerated much more rapidly than the slowly moving ions. The ions travel across the tube and eventually strike the cathode. When they do so, they release a could of secondary electrons from the material in the cathode. These electrons are accelerated back toward the anode. If the voltage enough, when these high-energy electrons collide inelestically with neutral atoms they create more ions. This process of secondary electron release and ion creation sustains the plasma. (Campel 2001)

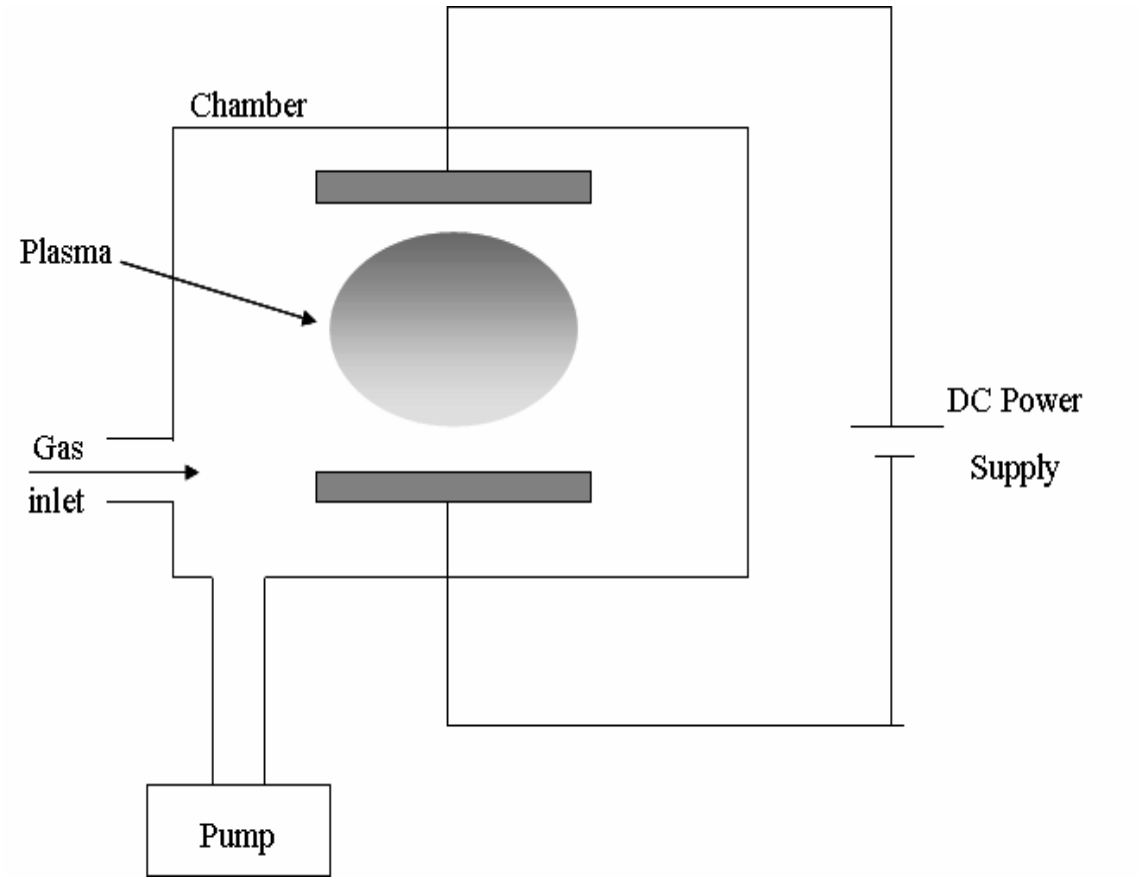

Figure 2.2. Basic schematic of dc glow discharge

Sputtering is a phenomenon occurs from the interactions between the surface atoms and the incident atoms. The interactions between the incident particle and the target surface are mostly dictated by the kinetic energy of the incident particle. When an energetic ion strikes the surface of a material, four things can be happened.

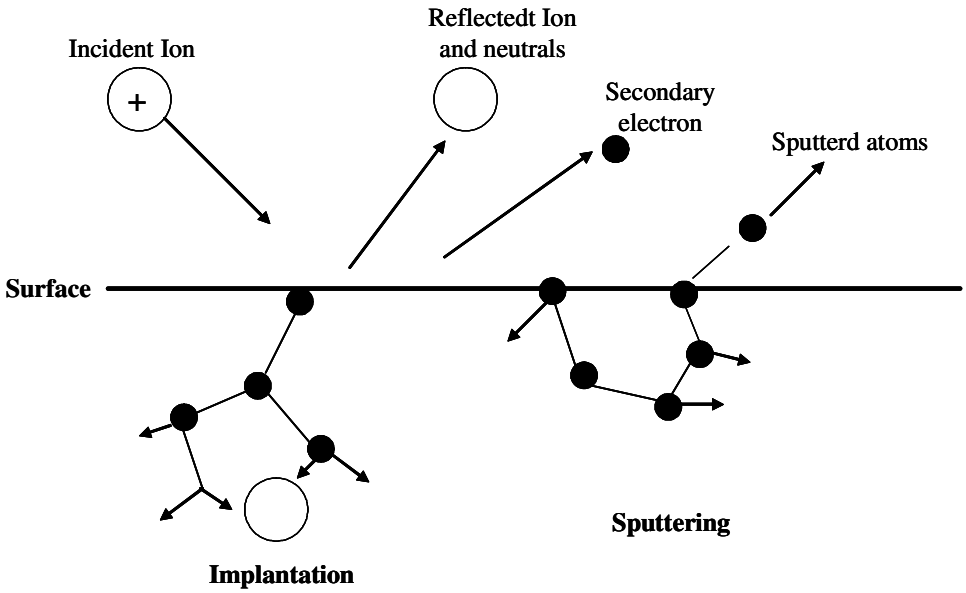

Figure 2.3. Possible outcomes for an ion incident on the surface of a solid

As shown on figure 2.3, at the energies of less than about 10 eV, the ion may also adsorb to the surface, giving up its energy to phonons (heat). At energies above about 10 keV, the ion penetrates in to the material many atomic layer spacing. It changes the physical structure of the surface. This high energy is typical for Ion Implantation. The kinetic energy of interest of the incident particles for sputter deposition is an order of larger than the binding energy of the surface atoms (10 and 40 eV) and lies between 100 and 1000 eV. In this energy range, momentum is transferred from the incident particle sequentially to the atoms in the near surface region of the target.

The sputter yield, S, which is the removal rate of surface atoms due to ion bombardment, is defined as the number of emitted particles from solid surface(target) per incident ion and given by:

$$S = (\#\text{ of emitted particle}) / (\#\text{ of incident ion}) \qquad (2.2)$$

The energy and the angle of the incident particle, relative masses of target and bombarding species, surface morphology and the purity of the target will influence the sputter yield.

2.3.1. Sputtering Systems

There are several sputtering systems for thin film production. These are dc diode, rf diode and magnetron sputtering. Among these sputtering systems, the basic model is the dc diode sputtering system. The other sputtering systems are improvements on dc diode sputtering system. In our study, we used a magnetron sputtering system. Here, the magnetron sputtering system will be discussed.

2.3.1.1. Magnetron Sputtering

Low pressure sputtering is one of the promising techniques for the production devices based on thin films. Low pressure sputtering will suggests high deposition rates due to the large mean free path for sputter atoms.

$$m\frac{d\mathbf{v}}{dt} = q(\mathbf{E} + \mathbf{v}\times\mathbf{B}) \tag{2.3}$$

Motion of a charged particle in the presence of a magnetic field and electric field is described by Lorent`z famous formula given in Eq.3. According to this formula electron motion follows a helical trajectory around the magnetic field lines, with an imposed drift known as the E×B drift. This property can be used to contain electrons in the discharge above the cathode to improve the collision probability of electrons with gas molecules.

A magnetron uses a static magnetic field configured at the cathode location. Secondary electrons which are emitted from the cathode surface due to the ion bombardment are constrained by this magnetic field to move in a direction perpendicular to both magnetic and electric field. Different from the dc and rf diodes, these secondary electrons are trapped in region (drift ring) close to cathode. These trap electrons increases the probability of ionizing collisions. Ions which are made in the

drift region hit the cathode. This results in even more generation of secondary electrons and extremely dense plasma in this drift region. The location of this ring is also known as the etch track because the erosion of the cathode is highest here due to the extremely dense plasma.

Secondary electrons emitted from the cathode surface are trapped in the drift track and make ionizing collisions with sputtering gas molecules (generally Ar). The resulting Ar^+ ions hit the cathode and provide the emission of more secondary electrons and sputter of cathode (target) atoms. Containment of the secondary electrons in the drift track leads to an extremely dense plasma and therefore a higher ion current and deposition rate. This leads to a lower sputtering gas pressure and discharge voltage compared to dc and rf diode systems in magnetron sputtering system. The sputtering gas pressure in magnetron sputtering systems is as low as 10^{-5} Torr. This low pressures leads to enhance in mean free path of the sputter atoms of the target material.

In figure 2.4, a new magnetron sputtering head configuration is shown. E field is created between shield and target material. Rare magnets create the constant magnetic field. The bias voltage is not used. This configuration is used in our magnetron sputtering system.

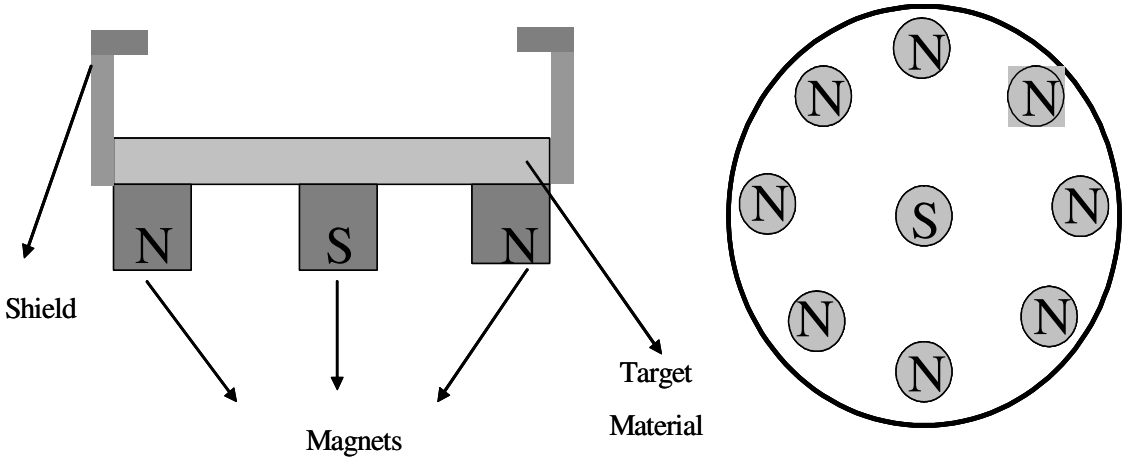

Figure.2.4. A view of magnetron sputtering configuration

2.4. MgB_2 thin Films

2.4.1. Growth Methods

In this section, we provide a general description of MgB_2 film growth methods. It is important to know the phase diagrams of MgB_2 because there is very large imbalance between the vapor pressure of Mg and B. Mg is highly volatile element and B has a high melting temperature. The phase diagrams of the MgB_2 were showed by Liu *et al* (Liu et al. 2001) based on thermodynamic of Mg-B binary compounds. In the Mg-B system, there are three intermediate compounds, MgB_2, MgB_4 and MgB_7, in addition to the gas, liquid and solid magnesium phases and the solid boron phase. These characteristic properties of MgB_2 are very important for a suitable growth of MgB_2 thin films. Deposition of MgB_2 thin films has some problems. One of them is the high oxidation sensivity of Mg. Mg is very volatile material. It starts to oxidation at low temperature even at room temperature. This value limited some annealing procedure in some deposition systems. Other main problem is high vapor pressure of Mg.

In order to overcome the main difficulties of MgB_2 thin films growth, several methods were developed. Most commonly used technique is Pulsed Laser Deposition system (PLD). (Brinkman et al. 2001, Mijatovic et al. 2005, Shinde et al. 2001, Zeng et al. 2001, Chen et al. 2002, Ionescu et al. 2002). Brickman's group grown epitaxial MgB_2 films for SQUID applications has T_c ~37 K. These films have large critical current about $5x10^7$ A/cm^{2}at 4.2 K. They used an Ar/H gas mixture during the deposition, to decrease the oxidation of Mg. Shinde's group examined the in-situ and ex-situ annealing process of grown films by PLD. For ex-situ process, they prepared the boron films by PLD annealed at 900 ^oC with excess Mg. Their films show the transition ~ 39 K for ex-situ process. In the in-situ process, they used a stoichiometric target to deposit MgB_2 thin films with a T_c ~ 22 K at high substrate temperature. They explained that this low transition temperature is loss of Mg at high temperature. Zeng et al showed a low temperature in-situ annealing process at 200 ^oC-300 ^oC. Their zero resistance temperature is ~34 K and with ~1.34 x 10^6 A/cm^2 J_c at 7.2 K. These results and other studies showed that a PLD deposition technique is suitable for high critical temperature; nearly bulk T_c, MgB_2 thin film growth used in electronic applications.

Generally, in-situ growths are done in Ultra High Vacuum (UHV) systems, like a molecular beam epitaxy (MBE) (Ueda and Naito 2001, Harada et al. 2004). Ueda reported the growth temperature, thickness dependence, effects of excess Mg, and effects of in-situ annealing. In these studies, films were grown on suitable substrate by MBE system at ~ 300 ^{o}C. Transition temperature of the MgB_2 films grown by this group is ~35 K. Some groups reported that the best deposition temperature is between 200 ^{o}C-300 ^{o}C for good quality MgB_2 thin films (Jo et al. 2002, Erven et al. 2002). Jo et al prepared film showed the T_c at 34.5 K and they showed a big critical magnetic field value, 15 T, at 20 K ever reported.

In addition to these growth techniques, evaporation method is another important technique. Generally, a boron layer is grown by an evaporator, and then a post annealing process was performed in Mg vapor (Moon et al. 2001). This type films that have 10^7 A/cm^2 critical current density at 15 K showed ~39 K transition temperature. Another study is about reactive evaporation (Moeckly and Ruby 2006) method. They achieved to grow MgB_2 thin films on 4 inch *r*-plane sapphire substrate with T_c values ~38 K and ~39K. Zhang and his group used an e-beam evaporation method with an in-situ annealing process at 630 ^{o}C (Zhang et al. 2006). They also deposited precursor film Mg and B then deposited films before applying in-situ annealing. The growing films showed 24.5 K or 30 K transition temperature according to used substrate. The best technique for the chemical vapor deposition was hybrid physical-chemical vapor deposition (HPCVD) by Zeng et al, and Pogrebnyakov's group in Penn State (Pogrebnyakov et al. 2003, and Zeng et al. 2003). They used a special design for deposition the MgB_2 thin films by using reactive B_2H_6 gas mixture. The growing films by using HPCVD system have a zero resistance temperature at 39 K. Their high crystalline films have 1.2 x 10^7 A/cm^2 critical current at 4.2 K. Hence, co-evaporation methods are generally used to solve Mg vapor pressure problem.

Several studies were done by sputtering system to prepare the best quality MgB_2 thin films. These studies include in-situ and ex-situ annealing processes. (Bu et al. 2002, Vaglio et al. 2002). In these studies, different ways were used to deposit MgB_2 thin films. Bu et al deposited B layer by using a magnetron sputtering system than they annealed this film under Mg vapor. Their films showed good crystalinty c-axis oriented with 35 K transition temperature. Vaglio group used a planar magnetron sputtering at UHV condition to prevent Mg from oxidation. The grown films show good quality superconducting properties. Their transition temperature is 35 K with a high critical

current density value. Main problem is for a magnetron sputtering system to product MgB_2 thin films is a single MgB_2 target production. Generally two sputtering targets were used to deposit films; those are Mg and B targets (Ahn et al. 2003, Mori et al, 2004). This process called co-sputtering methods. After an in-situ anneal process at 600 ^oC, grown films by Ahn group reported T_c about 24 K. By using a Mg and B target, Mori group deposited the films, T_c is 24 K, with a RF magnetron sputtering system under two step annealing process. Some groups tried to develop a single MgB_2 target for a sputtering system. Akinaga (Akinaga 2003) used a Mg disc and many small chunks of B to perform a single MgB_2 targets. They used a RF sputtering system to deposit MgB_2 films from hand-made target. Their films show transition at low temperature around 15 K. Some groups tried to develop the ex-situ process for magnetron sputtering system (Wu et al. 2004, Ermolov et al. 2001, and Mancini et al 2003). They prepared the MgB_2 thin films by using a single MgB_2 targets, and then they tried to enhance the superconducting properties and to develop the crystal quality of the as-grown films by a post annealing condition. Wu et al prepared films showed a superconducting transition at below 25 K after ex-situ annealing process under 600 ^oC – 700 ^oC temperatures. Mancini reported a transition at ~27 K with a poor crystallinty after ex-situ process below 600 ^oC. Generally MgB_2 thin films grown by magnetron sputtering did not show perfect crystal structure or high T_c values, about ~39 K, but sputtering system is available to product large area thin film formation.

2.4.2. Substrates for MgB_2 Thin films

To deposit best quality thin films, the substrate choice is an important parameter. As mentioned in previous sections, the lattice mismatch parameter and reaction between deposited thin film and substrate affect the thin film formation.

MgB_2 has a hexagonal crystal structure mentioned in previous section. To grow good quality crystal MgB_2 thin films, the lattice parameters of substrate have to be matched with MgB_2 lattice parameters. Several substrates were examined to deposit best crystal thin films. Generally, Al_2O_3-R, Al_2O_3-C, MgO (100), $SrTiO_3$ (100), SiC (0001) and $LaAlO_3$ (001) are used. As mentioned above, MgB_2 has a hexagonal AlB_2 structure; it should prefer substrate with a hexagonal face. These substrate parameters were shown in Table 2.1 (Naito and Ueda 2003).

In addition to this interdiffusion or reaction between film and substrate were studied by He group (He et al. 2002). They reported the reactivity of MgB_2 powder with YSZ, MgO, Al_2O_3, SiO_2, $SrTiO_3$, AlN, Si and SiC. Table 2.2 shows the reactivity of MgB_2 with various electronic materials.

Table 2.1. The crystal structure and lattice constants of MgB_2 and several widely used substrates.

Substrate	Crystal System	a (A°)	c (A°)	Surface (lattice constant (A°))
$SrTiO_3$	Cubic	3.905		(100) Square (3.905)
$LaAlO_3$	Cubic	3.085		(001) Square (3.085)
MgO	Cubic	4.21		(100) Square (4.21)
Si	Cubic	5.431		(100) Square (5.43) (111) Hex. (4.76)
Al_2O_3	Hexagonal	4.76	12.99	C Hex. (4.76) R Rectangular
SiC	Hexagonal	3.081	15.12	(001) Hex. (3.081)
MgB_2	Hexagonal	3.086	3.552	(001)

Table 2.2. The reactivity of MgB_2 with various electronic materials.

Electronic Material	600 ^oC Anneal	800 ^oC Anneal
YSZ	No Reaction	MgB_2, small amount of MgO
MgO	No Reaction	No Reaction
Al_2O_3	No Reaction	MgB_2 with altered size, MgO
SiO_2	MgB_2, MgO, Si	MgB_2, MgB_4, MgO, Mg_2Si
$SrTiO_3$	No Reaction	MgB_2, $SrTiO_3$, MgO, SrB_6
Si	MgB_2, Mg_2Si	MgB_2, MgB_4, Mg_2Si
SiC	No Reaction	MgB_2 with altered cell size
AlN	No Reaction	No Reaction

CHAPTER 3

EXPERIMENTAL

In this study, we reported the production of a MgB_2/Mg composite sputtering target and the deposition of MgB_2 thin films using a high vacuum dc magnetron sputtering system. After deposition, an ex-situ process was performed to develop the superconducting properties of as-grown films. In this chapter, preparation of a MgB_2/Mg magnetron sputtering target, thin film preparation procedure, annealing process and characterization techniques will be explained.

3.1. Material

In this study, commercially available MgB_2 powder obtained from Alfa Aesar (31-44 micron average particle size, 98.5% purity) and Mg powder obtained from Alfa Aesar (31-44 micron average particle size, 99.99%) purity were used. The X-Ray diffraction patterns of used MgB_2 and Mg powders were given in Figure 3.1. The MgB_2 powder has a purity of 98.5% and the residual 1.5% MgO. Mg powder has purity 99.99%. Any MgO peaks were not detected in XRD patterns of Mg powder.

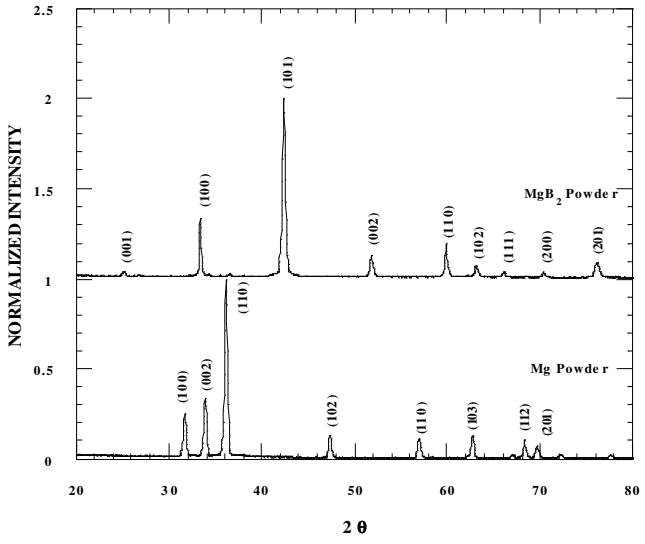

Figure 3.1. XRD patterns of MgB_2 and Mg powder

3.2. Experimental

In this section magnetron sputtering target production steps, thin film preparation and post annealing procedures will be discussed**.**

3.2.1. MgB_2 / Mg Sputtering Target Preparation

In this study, we prepared a MgB_2/Mg composite target. The commercially available MgB_2 and Mg powders were used for the fabrication MgB_2 / Mg composites. The weight ratio of Mg to MgB_2 was 20% for composites. MgB_2 and Mg powders were mixed homogenously and uniaxially pressed under pressure of 0.5 GPa in a metallic dye. The dye was heated to 500 ^oC and kept at the temperature for 1 hour in air. Figure 3.2 shows the MgB_2 pellet production steps. The temperature was controlled with a variac and a thermocouple connected to Omega temperature controller.

Based on previous studies oxidation of MgB_2 in air begins at 400 ^oC, however oxidation is not expected to be very strong less than 700 ^oC (Yung et al. 2003). Therefore selected temperatures for MgB_2/Mg composite pellets are convenient to prevent the oxidation of MgB_2 to MgO. Melting point of Mg is 654 ^oC. Hence, no preponderant oxidation reaction is excepted for Mg at selected temperatures especially for 500 ^oC. Previous studies discussed preparation of MgB_2/Mg composites in detailed (Egilmez et.al. 2006). As we know, Mg is volatile material. It is more sensitive to oxidation even at low temperature. We discussed some growth difficulties of the MgB_2 thin films in chapter 2. In addition to this, Fan et al reported the decomposition of the MgB_2 during the deposition according to pressure of environment and Mg vapor pressure characteristic (Fan et al. 2001). When the magnetron sputtering target was prepared, in order to prevent loss of Mg during the deposition of thin films, we added Mg to MgB_2 (20% + 80%).

20 pellets in dimension with 1.5 cm diameter and 0.3 cm height were fabricated for the target preparation. Fabricated MgB_2/Mg pellets were cut in a shape to stick on a Mg disc by a silver paint. Mg disc was used to adjust the dimension of sputtering target for our system configuration. The Figure 3.3 and 3.4 show the prepared target schematic and photograps.

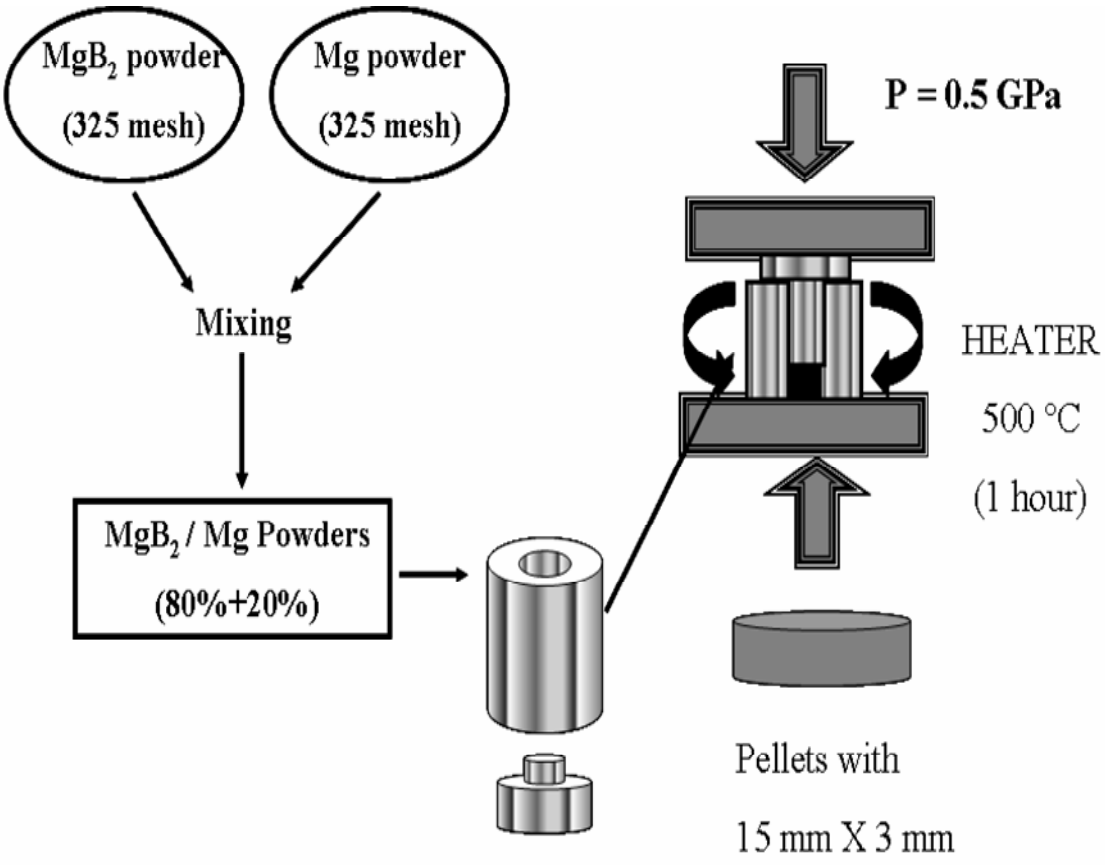

Figure 3.2. Experimental set up for pellet preparation

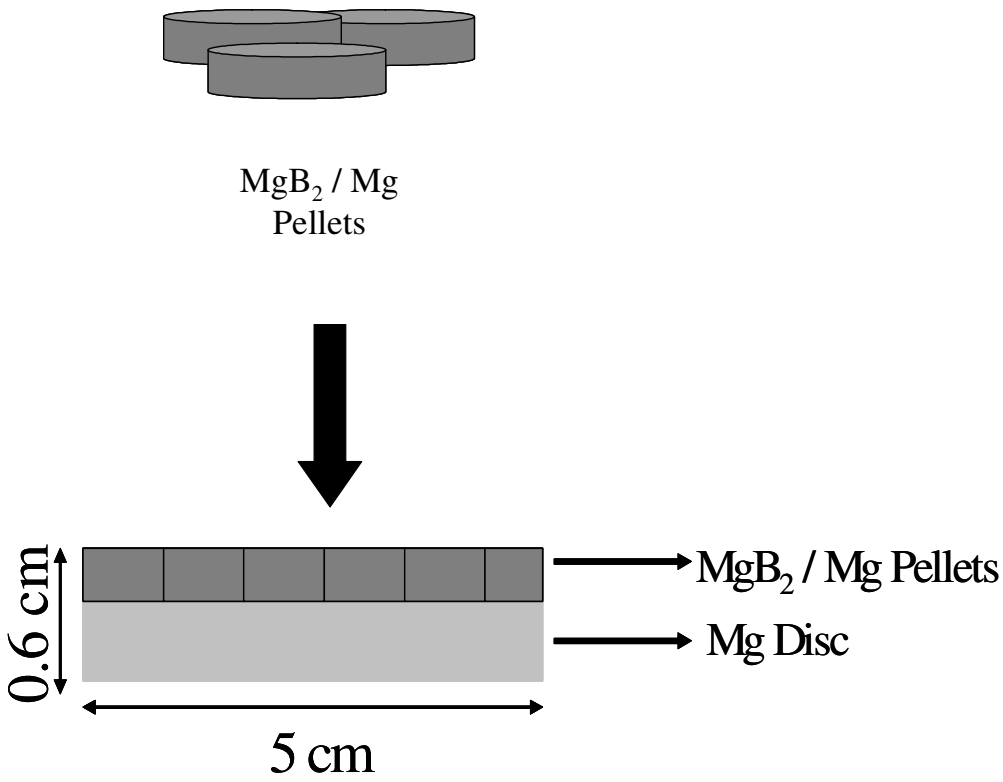

Figure 3.3. MgB_2/Mg pellets sticked on Mg disc

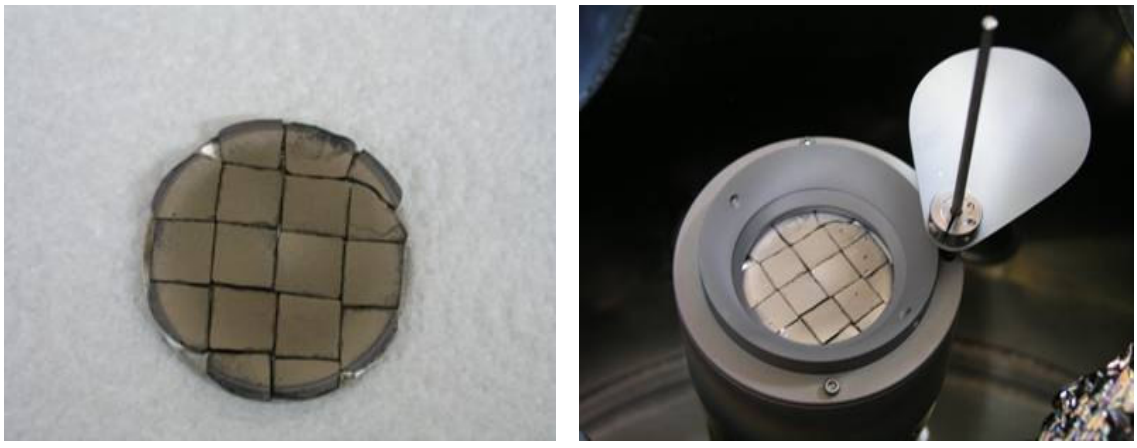

Figure 3.4. MgB_2/Mg target top view and located in sputtering head.

3.2.2. MgB_2 Thin Film Deposition System

Magnetron sputtering system that is used in experiment is a High-Vacuum system shown in figure 3.4. A rough pump and a turbo molecular pump (TMP) were used to approach a high vacuum region. To measure base pressure of the system, a thermocouple and an ion gauge were used. Magnetron sputtering system has 4 guns with a water cooling channel, gas entrance and power connections. To measure pressure of the vacuum chamber during the deposition, a MKS type Baratron was used. Gas flow was controlled by a MKS mass flow controller. A gate valve with a stepper motor was connected to the system in front of TMP. An Advanced Energy dc Power supply was used. The Figures 3.5 and 3.6 represent the picture of used magnetron sputtering system in our thin film laboratory and schematic of the magnetron sputtering system.

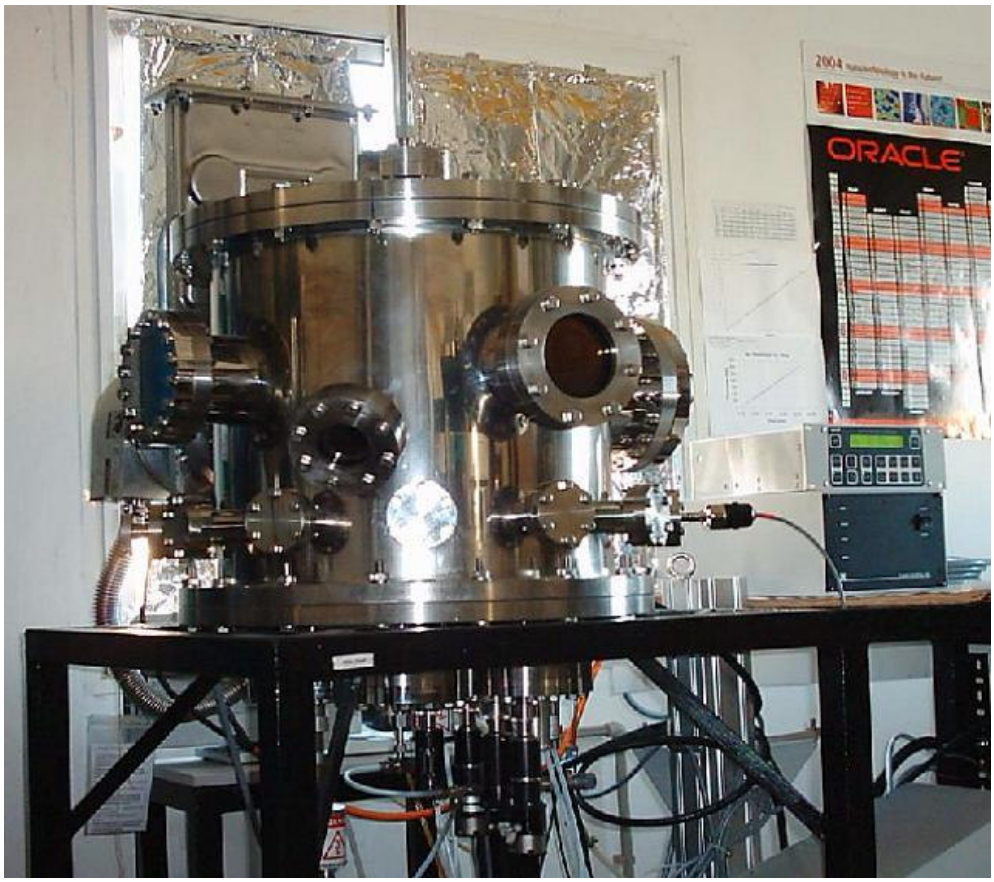

Figure 3.5. Picture of the magnetron sputtering system

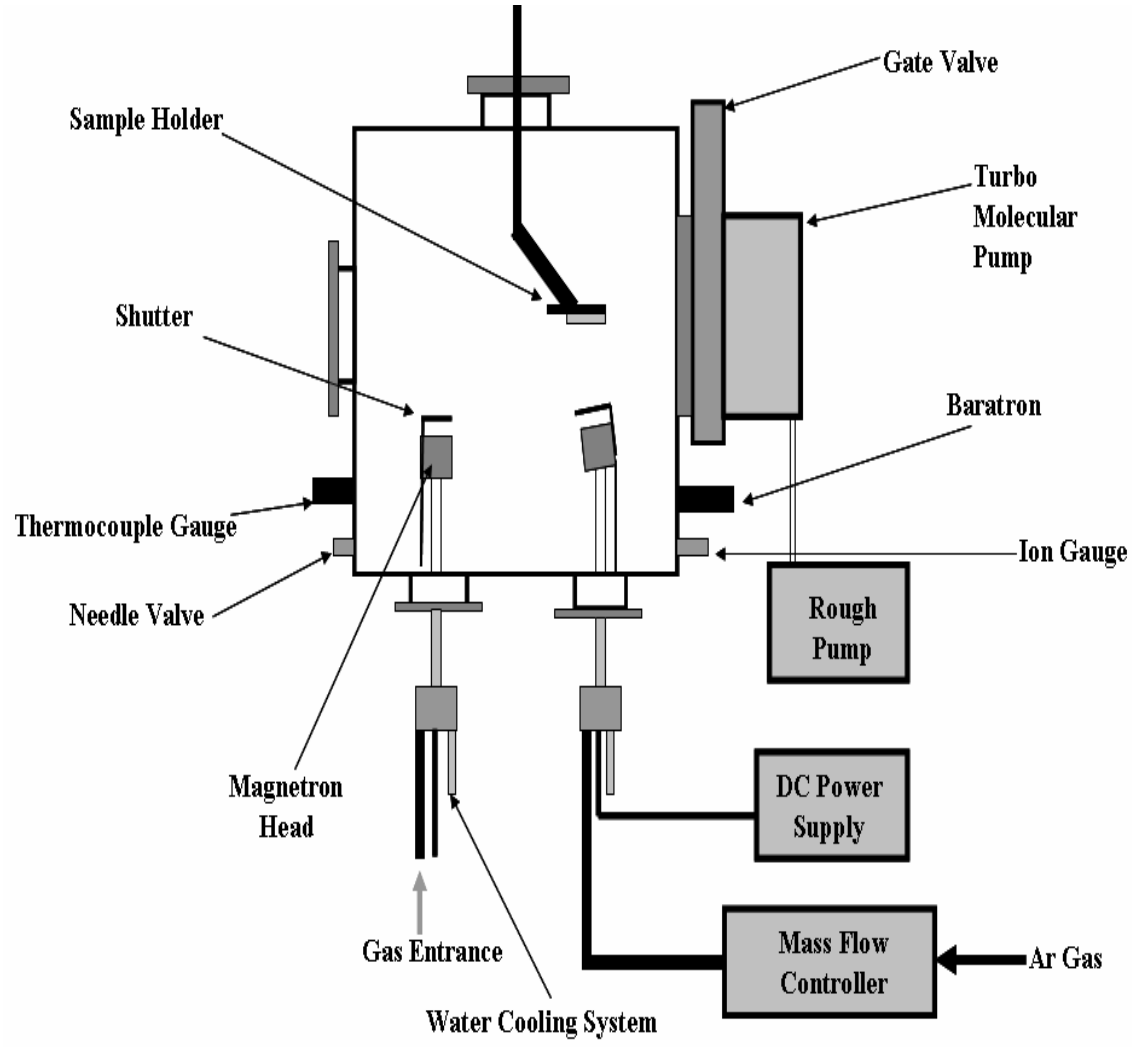

Figure 3.6. Schematic of the Magnetron Sputtering System

3.2.3. MgB_2 Thin Film preparation steps

3.2.3.1. MgB_2 Thin Film Deposition

An Al_2O_3 polycrystal and a $LaAlO_3$ (001) single crystal substrates with a dimension 0.5 cm X 1.5 cm X 0.1 cm were used to grow MgB_2 superconducting thin films. A high vacuum magnetron sputtering system was used to grow MgB_2 thin film on these substrates in department of physics at Izmir Institute of Technology, Turkey.

Firstly, as known, cleaning of the substrate is very important step for growth of thin film. All substrates were cleaned with a chemical process. This process includes that 10 minutes pure water cleaning first, and then 15 minutes acetones and 10 minutes pure water cleaning again by a vibrating water bath. After that, cleaned substrates were dried in an Ar gas flow to remove pure water on the substrate after cleaning process. Finally, cleaned substrates were loaded to vacuum chamber.

System was pumped by using two different vacuum pumps, these are rough pump (below to 10^{-3} Torr) and a TMP (below 10^{-6} Torr). The base pressure was below $2.0x10^{-6}$ Torr. Ar gas (purity 99.99%) was used as an inert gas. After reached to base pressure, 20 sccm Ar gas was flowed to the chamber by using a mass flow controller. At the same time the gate valve closed to 40% of its fully open position. During the process, deposition pressure was 2.5 mTorr.

Depositions were done in two steps, the first one is a pre-sputtering step and the second one is a thin film deposition step. To remove contamination of target surface a pre-sputtering step was performed. In this process, pressure was 2.5 mTorr (20 sccm Ar gas and 60% valve is closed), 30 W powers and 72 mA current were applied to the target by using a dc power supply for 30 minutes, as the shutter of the magnetron sputter head was closed. Then, shutter was opened and the power was increased to 50 W, applied current to the target was 120 mA. Deposition time of the MgB_2 thin films were 3 hours. We prepared the MgB_2 films at room temperature. It means that any substrate heater was not used to heat substrate. Substrate distance from the target surface was constant for all experiments.

After deposition steps, the pressure of the chamber was reached to atmosphere pressure to remove the substrate holder from the chamber.

3.2.3.2. Post Anneal Step

As mentioned in chapter 2, there are several steps to produce the MgB_2 thin films. We used a two step film production called ex-situ process. The second step was annealing step which is called "ex-situ annealing".

To perform annealing process; a high temperature (~1200 ^oC) tube furnace was used. Deposited films by magnetron sputtering were put in a crucible and then they were located in a quartz tube in the middle of the furnace. During the anneal process Ar gas flowed in quartz tube to prevent the films from oxidation. Annealing process was run in two different duration and different temperatures, 20 and 30 minutes, 625 ^oC and 650 ^oC. The temperature of the tube furnace reached the annealing temperature with a rate of 20 ^oC/minute. These annealing temperatures were selected because of the evaporation temperature of Mg (654 ^oC). To remove the annealed sample from the furnace, it was waited that the system reached the room temperature (20 ^oC–30 ^oC). During the cooling process, Ar gas also flowed through the quartz tube. Figure 3.7 shows the basic schematics of annealing system.

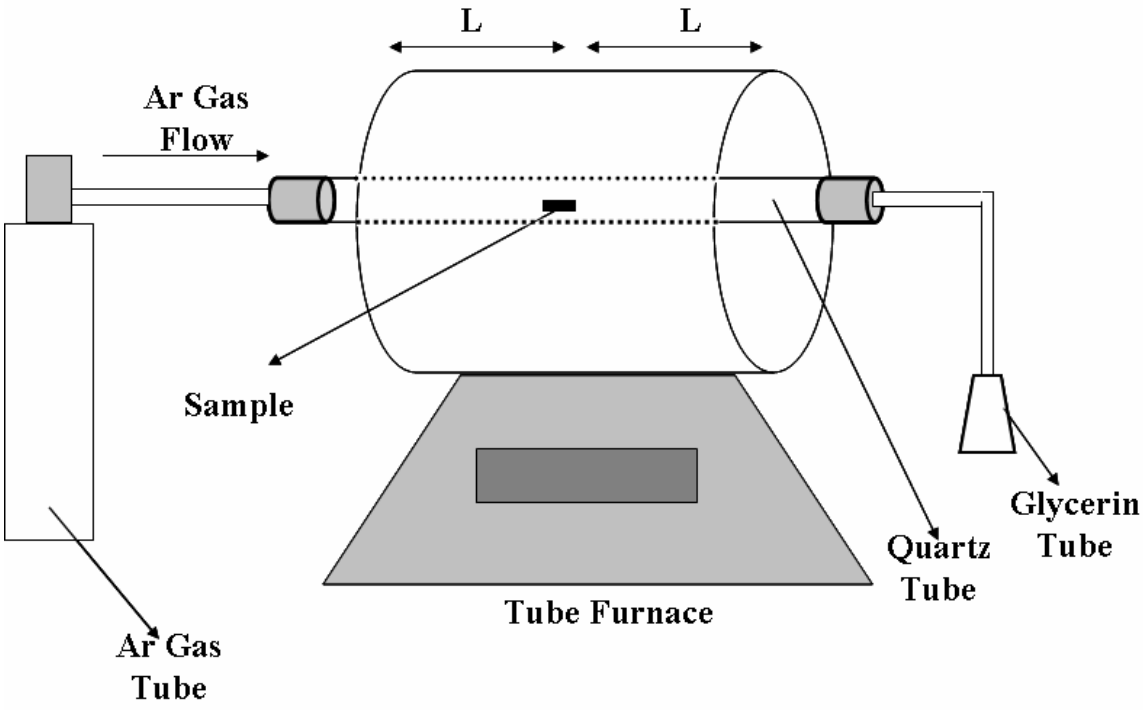

Figure 3.7. Schematic of the annealing system

3.3. Characterization and Measurements

3.3.1. X-Ray Diffraction Methods

X-Ray diffraction method is used to determine the crystal structure of the materials. To identify of the crystal structure of the MgB_2 thin films, X-Ray Diffraction method was used in this study. Grown MgB_2 thin films on Al_2O_3 polycrystal substrates were scanned in $2\Theta = 20^o$ to 80^o region. For the all samples, the run time was same. An X-Ray powder diffractometer with a CuK_α radiation with Ni filter adjusted to 45 kV and 40 mA (Phillips X'Pert Pro) was used in Material Research Center at İzmir Institute of Technology, Turkey.

3.3.2. Scanning electron Microscopy (SEM) and Electron Dispersive X-Ray (EDX) Analysis

Scanning Electron Microscopy techniques was used to determine the microstructure of the films and to obtain the surface morphologies of the grown films on Al_2O_3 polycrystal substrate. In order to compare the all samples, same magnification values for all characterization were used by SEM. Cross section images were taken to measure the thickness of the grown films on Al_2O_3 polycrystal substrate and $LaAlO_3$ single crystal substrate.

In addition to this analyzes, Electron Dispersive X-Ray (EDX) was used to investigate the chemical contents of the grown films. Mg, B and O contents were determined by EDX. For all samples, same electron energy was used to collect EDX data in correctly. A SEM (Phillips XL-30S FEG) was used in Material Research Center at İzmir Institute of Technology, Turkey.

3.3.3 Electrical Properties and Magnetic Properties

As known as, the main characteristics of the superconductor is zero resistance at below a certain critical temperature called T_c. To determine transition temperature of the prepared thin films, the traditional four-probe method was used. The films were cut in

the same dimensions (0.25 cm x 1.5 cm x 0.5 cm) by a diamond saw for the electrical measurements. In this method, the DC resistance of a sample is measured by a voltage drop across a specimen when a current of known magnitude.

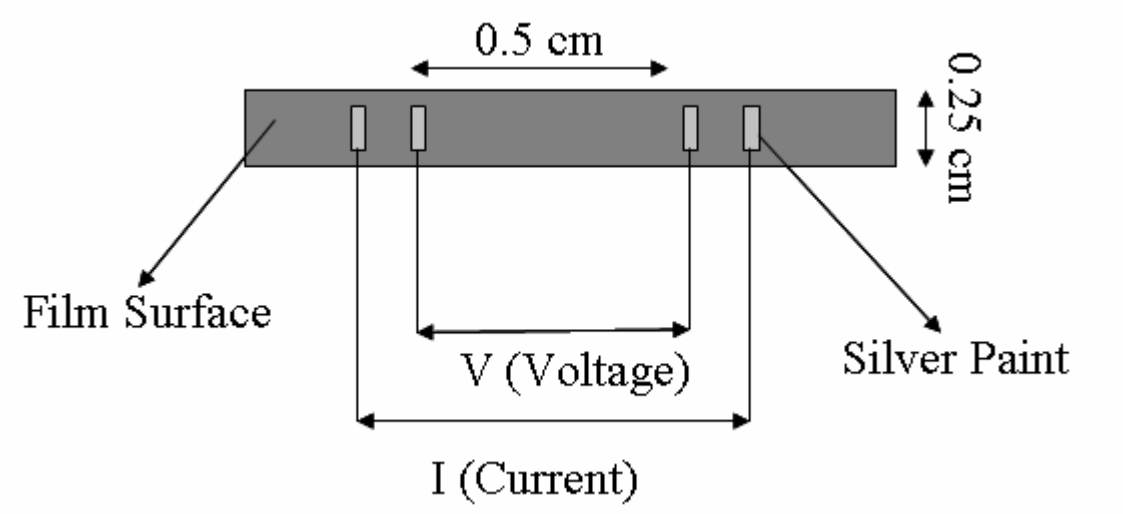

Figure 3.8. Schematic of four-point contacts

A current is applied at the outside contact, then the voltage drop between the inside contacts is measured with various temperature values. From this measurement, resistance & temperature, transition temperature, T_c of the superconducting materials can be founded.

In this study, in order to determine the transition temperature of the samples, a four point method was used. Figure 3.8 show a schematic of four point contacts on the film prepared for low temperature electrical measurements. A typical applied current is 1 mA. The voltage drops were measured between two points at inside. Temperature was changed room temperature (300 K) to low temperature (10 K). In addition to these measurements, temperature dependence resistance experiment was done in various magnetic fields which are applied perpendicular to the film surface, 0T, 3T, 6T. All four point measurements were performed at a Cryogenics Free Magnet System in Department of Physics at Inonu University, Malatya, Turkey.

CHAPTER 4

RESULTS AND DISCUSSION

Prepared MgB_2 superconducting thin films were characterized by XRD to determine the crystal structural. SEM-EDX characterization technique was used to obtain the surface morphology and chemical contents of the films. In addition to this, low temperature electrical measurements under various magnetic fields were performed to examine superconducting properties of the MgB_2 thin films. In this section of thesis; results of structure characterization and low temperature electrical measurements will be discussed.

4.1. XRD Results

The crystal structure of MgB_2 thin films prepared by a magnetron sputtering system were investigated by XRD patterns. In the beginning of the study, commercially available MgB_2 and Mg powders were used to produce a sputtering target. XRD patterns of these powders were shown in chapter 3. In this section, XRD results of prepared films will be discussed.

The intensity of each pattern is normalized to their maximum 2Θ values. All graphs were plotted normalized intensity to 2Θ values. Every sample was scanned between $2\Theta=20^{o}$-80^{o} region. In this study, all data was taken from grown films on Al_2O_3 polycrystal substrate.

As mentioned at the previous sections, MgB_2 has a simple crystal structure, hexagonal crystal structure. It should prefer substrate with a hexagonal face. Generally used substrates for growth of good crystal quality MgB_2 thin films were mentioned in chapter 2. An Al_2O_3 polycrystal substrate was used to grow MgB_2 thin films. To make better explanations for the XRD results, patterns of the Al_2O_3 substrate were taken. Figure 4.1 shows the XRD result of Al_2O_3 polycrystal substrate and its orientations.

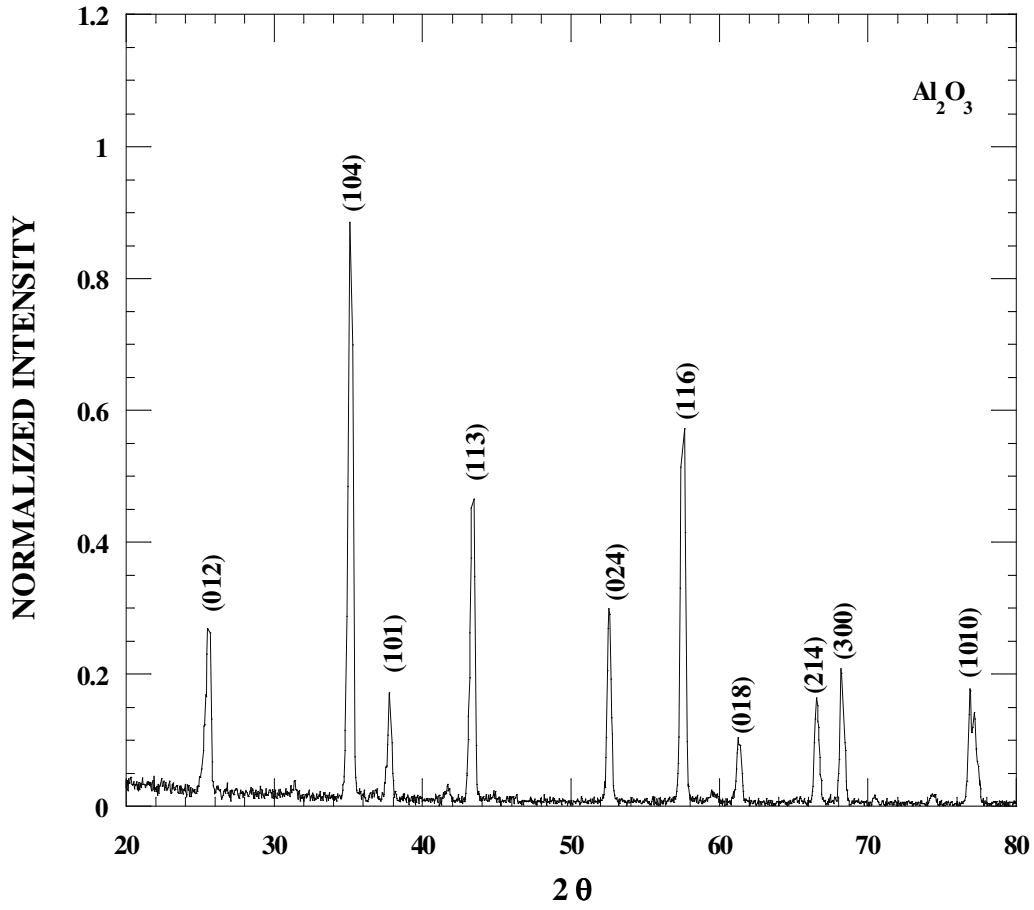

Figure 4.1. XRD pattern of Al_2O_3 substrate

Figure 4.2 shows the XRD data of MgB_2 film annealed at 650 ^oC at 20 min. sample and Al_2O_3 substrate. The curve at the top exhibits peaks of MgB_2 thin film annealed at 650 ^oC at 20 min. sample on Al_2O_3 polycrystal substrate, and the curve at the bottom shows the peaks of Al_2O_3 polycrystal substrate. In this figure, some shoulders were observed around $2\Theta = 42.5^o$ and $2\Theta = 62^o$ values. These peaks overlapped to the Al_2O_3 peaks occurring at the same positions at the XRD pattern. Therefore, they can not be clearly determined. When we compared the XRD results of polycrystal Al_2O_3 substrate and MgB_2 powder, we observed that their main peaks occur nearly at same 2Θ values in the XRD pattern. It is observed that they are overlapped to each other. To solve this problem and to make better analysis for the XRD results of the grown films, XRD pattern of Al_2O_3 polycrystal substrate was used as a background signal. Therefore, the substrate peak intensities were subtracted from XRD signal of MgB_2 films on Al_2O_3 substrate. Hence, at the end of subs traction, final signal just belonged to the MgB_2 thin films grown on Al_2O_3 substrate. After this calculation, it is easy to determine the films XRD results of the MgB_2 thin films.

Figure 4.3 shows the XRD results of as-grown film, substrate and subtraction results. The curve at the top exhibits peaks of as-grown MgB_2 thin films on Al_2O_3 polycrystal substrate, the curve at the middle shows the Al_2O_3 substrate and the curve at the bottom shows the signal that just comes from film grown on the Al_2O_3 polycrystal substrate after subtraction. As seen in Figure 4.3, any peaks were not detected in the XRD pattern after subtraction. There is no crystal peaks related to MgB_2 phase, Mg phase or MgO phase. It shows that as-grown film has totally amorphous structure. In this study, the starting materials, those are MgB_2 and Mg powders, showed crystal structure in their XRD patterns. We used them to product a sputtering target. Egilmez et al reported that MgB_2 pellets with 20% excess Mg prepared by hot press technique showed crystalinity. After deposition of films using prepared MgB_2 target from Mg and MgB_2 powders, as-grown films did not show any crystalinity. In order to increase the crystalinty of the as-grown MgB_2 thin films an ex-situ annealing processes were applied for as-grown MgB_2 thin films on Al_2O_3 polycrystal substrate.

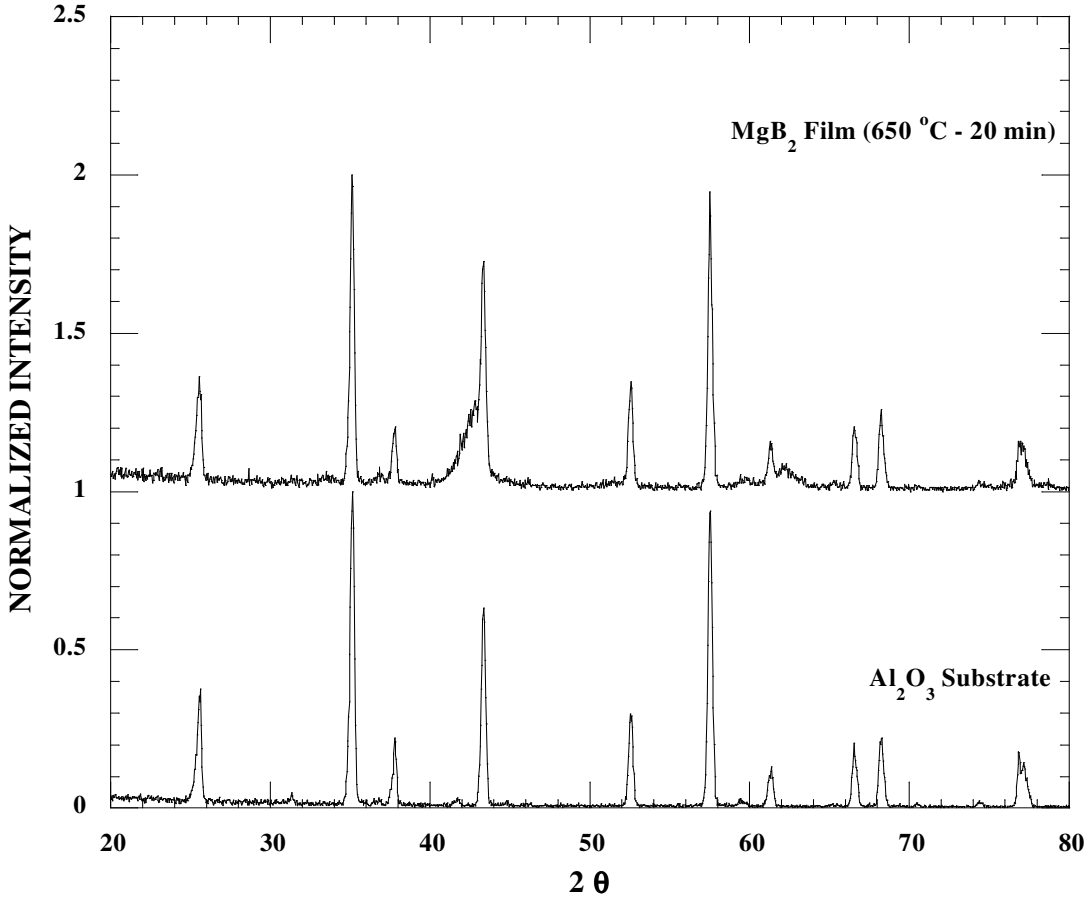

Figure 4.2. XRD patterns of 650 ^{o}C–20 min. annealed MgB_2 thin film-Al_2O_3 substrate

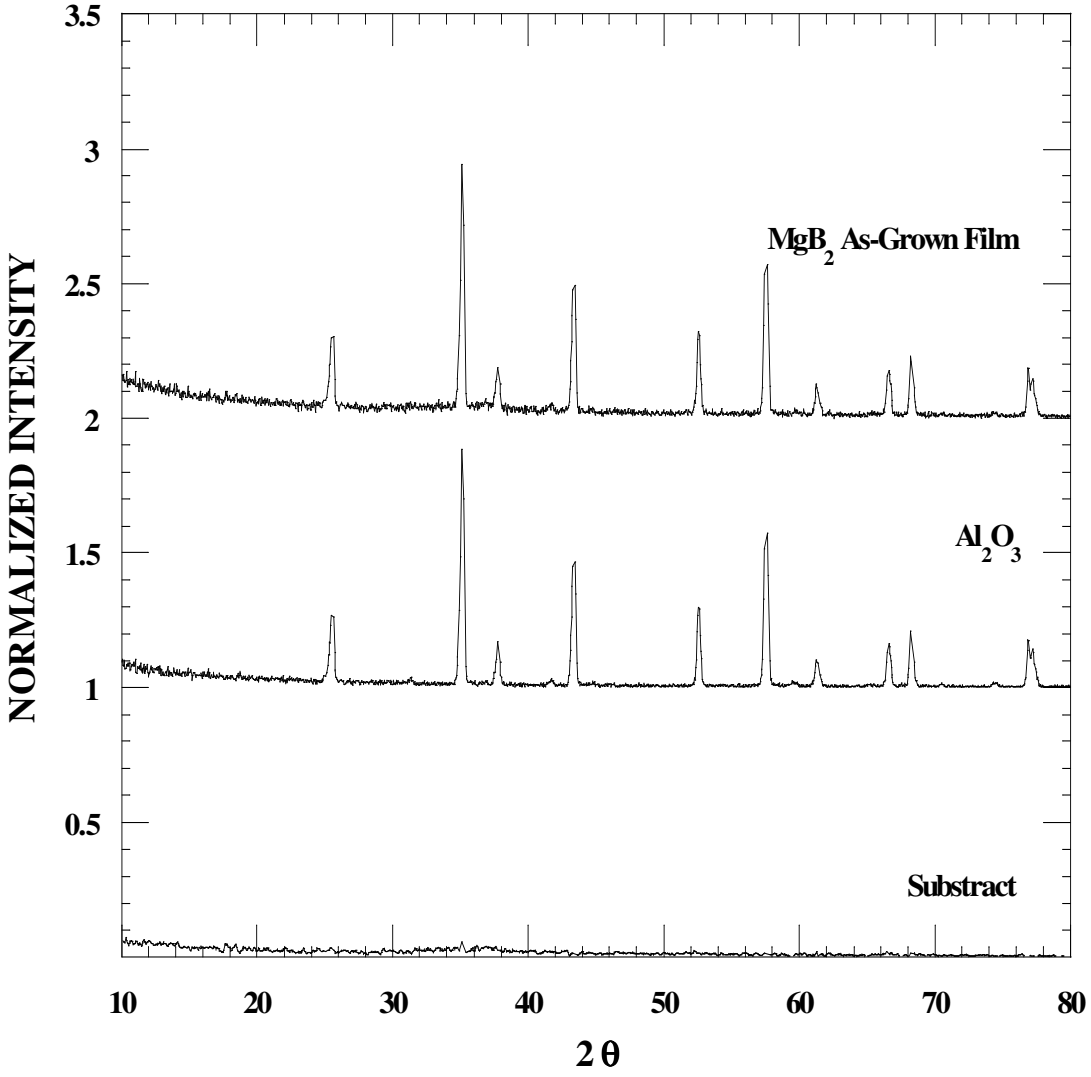

Figure 4.3. XRD patterns of as-grown MgB_2 thin film-Al_2O_3 substrate-subtract

The Figures 4.4 to 4.7 show the XRD results of annealed films; 625 ^{o}C-20 min., 650 ^{o}C-20min., 625 ^{o}C-30min., 625 ^{o}C-30min., 650 ^{o}C-30min. respectively. In order to compare the XRD results of the prepared thin films with the XRD results of MgB_2 powder, each graph includes the XRD patterns of MgB_2 powders.

It can clearly be said that the crystalinity of the samples starts after ex-situ anneal process. The main peak of MgB_2 (101) that is observed at $2\Theta=42.5^{o}$ occurs as the main phase in all annealed films. In addition to this main phase, a MgO peak at $2\Theta=62.2^{o}$ can be observed in all films as a second main phase. It shows that annealing process increase the crystalinity of the MgO phase in prepared films.

From Figure 4.4, 625 ^{o}C-20 min. annealed sample, we can observe a poor crystalinty at $2\Theta=33^{o}$, $2\Theta=51.8$, and $2\Theta=76.16$ related to MgB_2 phase. The peak of MgB_2 (102) at $2\Theta=63.2^{o}$ location is very close to MgO peak at $2\Theta=62.2^{o}$. The crystalinity occurring in this 2Θ position can include MgB_2 and MgO phases at the same time. It can be thought that these peaks can overlap to each other because of quality of peaks.

The 650 ^{o}C-20 min annealed sample showed same peaks mentioned above for 625 ^{o}C-20 min. annealed sample, but the peak occurring at $2\Theta=76.16^{o}$ related to MgB_2 (201) started to disappear in this sample. As a result of increasing annealing temperature, a new MgO crystal peak appeared at $2\Theta=43^{o}$, and at 650 ^{o}C-30 min. annealed sample this peak can be observed better than 625 ^{o}C-30 min sample. It shows that increasing the annealing duration change the crystalinty of the grown films. On the other hand, increasing the annealing temperature and duration parameters develop the quality of the main MgB_2 (101) peaks locating at $2\Theta=42.5^{o}$.In addition to these observations other Mg-B crystal phases are not observed, for instance MgB_4.

All in all, the main reasons of the MgO phase can be explained by two approaches. Firstly, we prepared the magnetron sputtering target from MgB_2 and Mg powders. During the hot press study in air, sputtering target pellets can include some porosity that means oxygen or any contamination. In addition to this, powders used in target preparation contain some impurity (1.5% MgO at MgB_2 powder).Secondly; we used Ar gas flow during the annealing process with purity 99.99%. It contains small amount of oxygen. As mentioned previous chapters, Mg is sensitive to oxidation even in at low temperatures. This is the main reason for MgO phase.

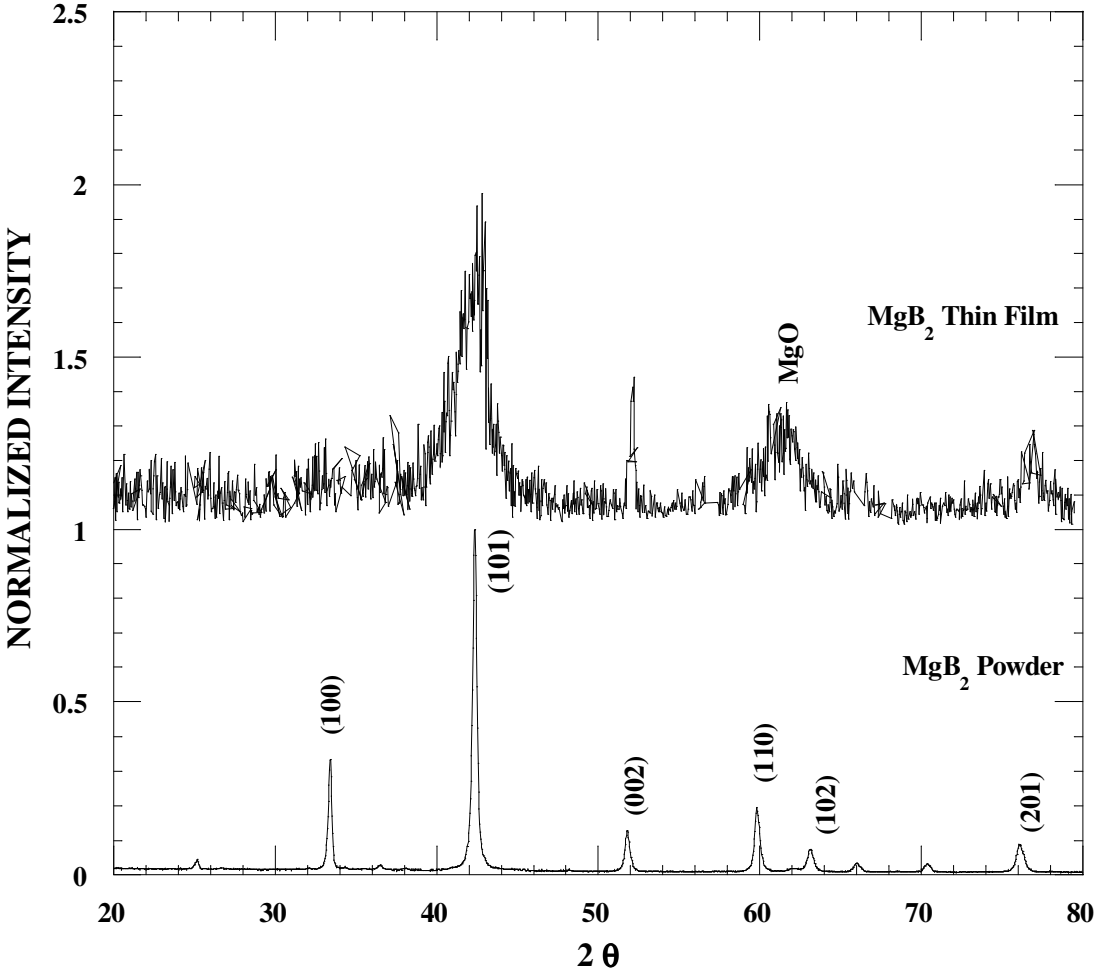

Figure 4.4. XRD patterns of 625 ^{o}C–20 min. annealed MgB_2 thin film - MgB_2 powder

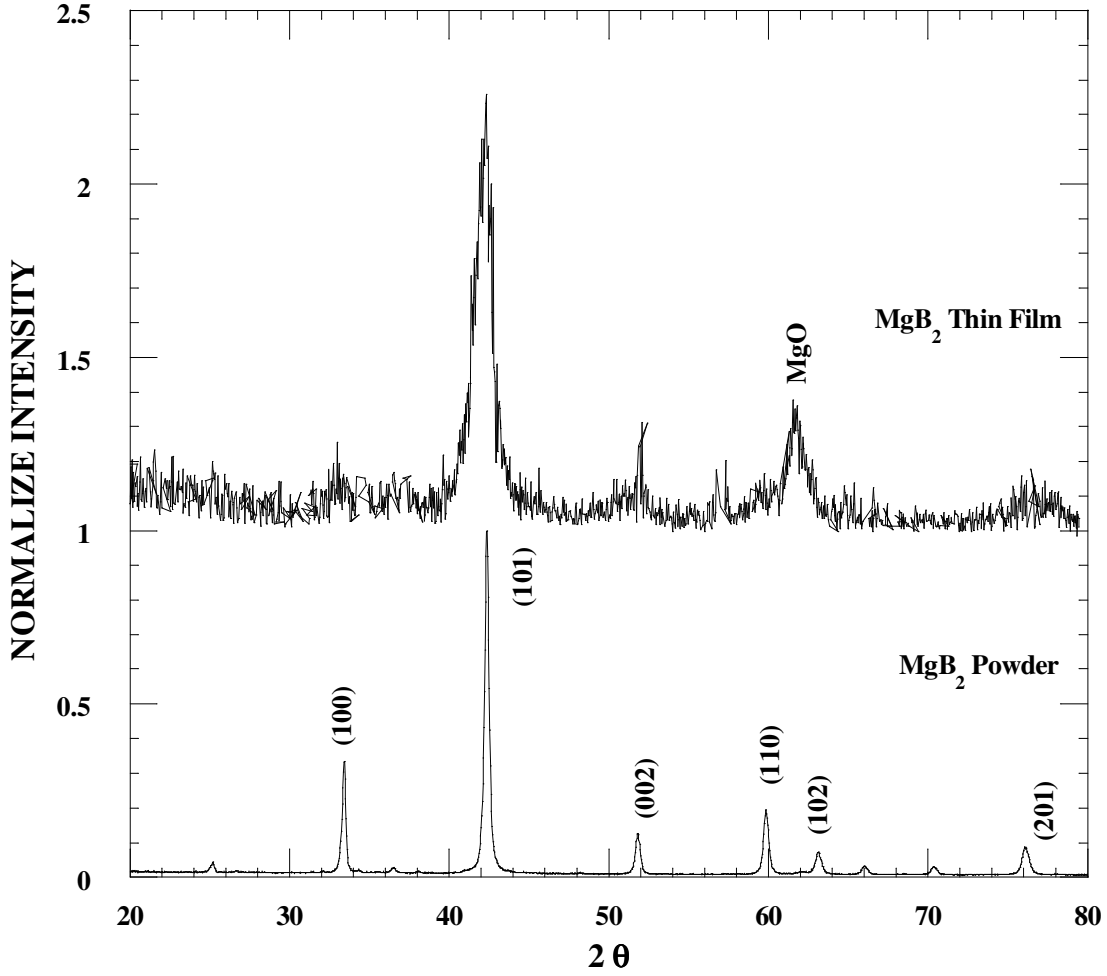

Figure 4.5. XRD patterns of 650 ^{o}C–20 min. annealed MgB_2 thin film- MgB_2 powder

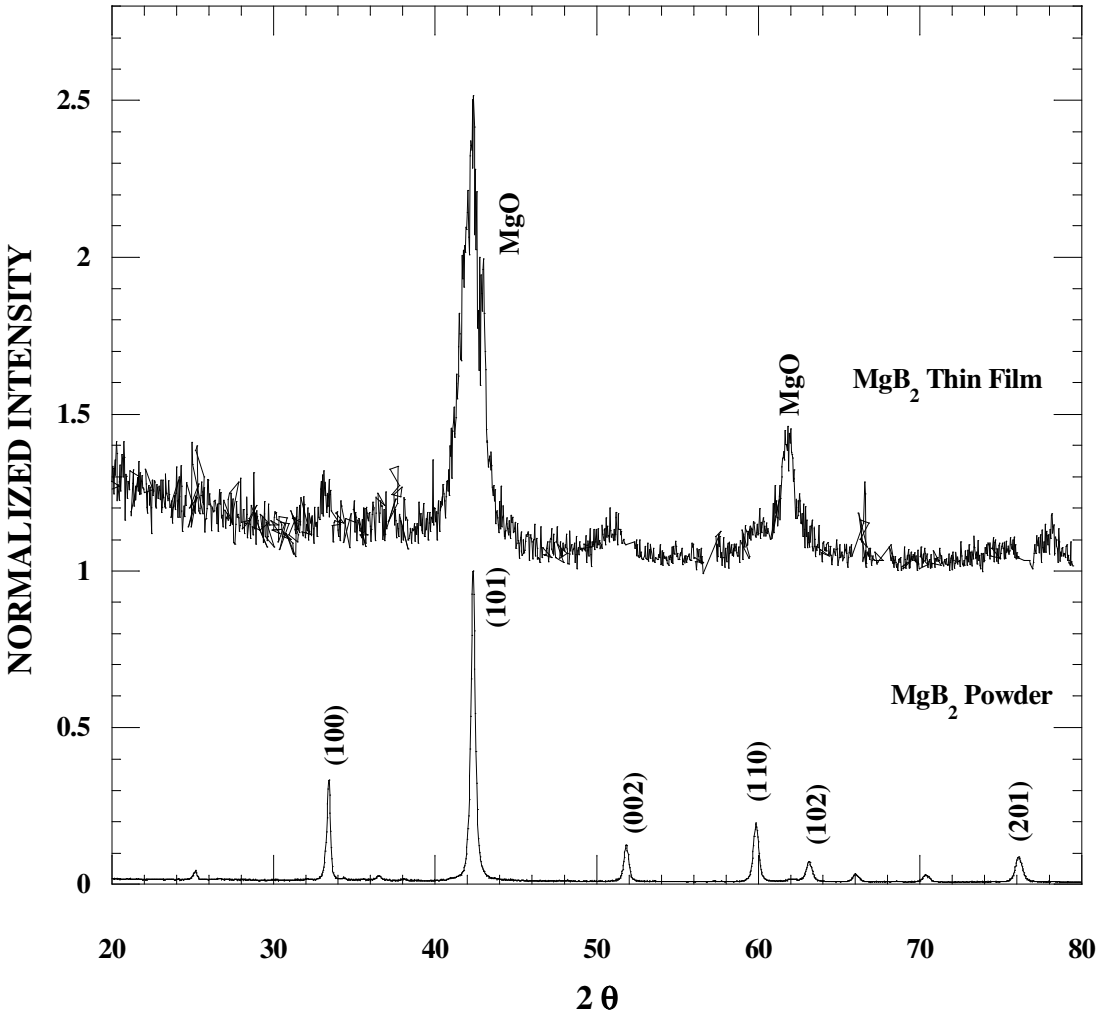

Figure 4.6. XRD Patterns of 625 ^{o}C–30 min. annealed MgB_2 thin film- MgB_2 powder

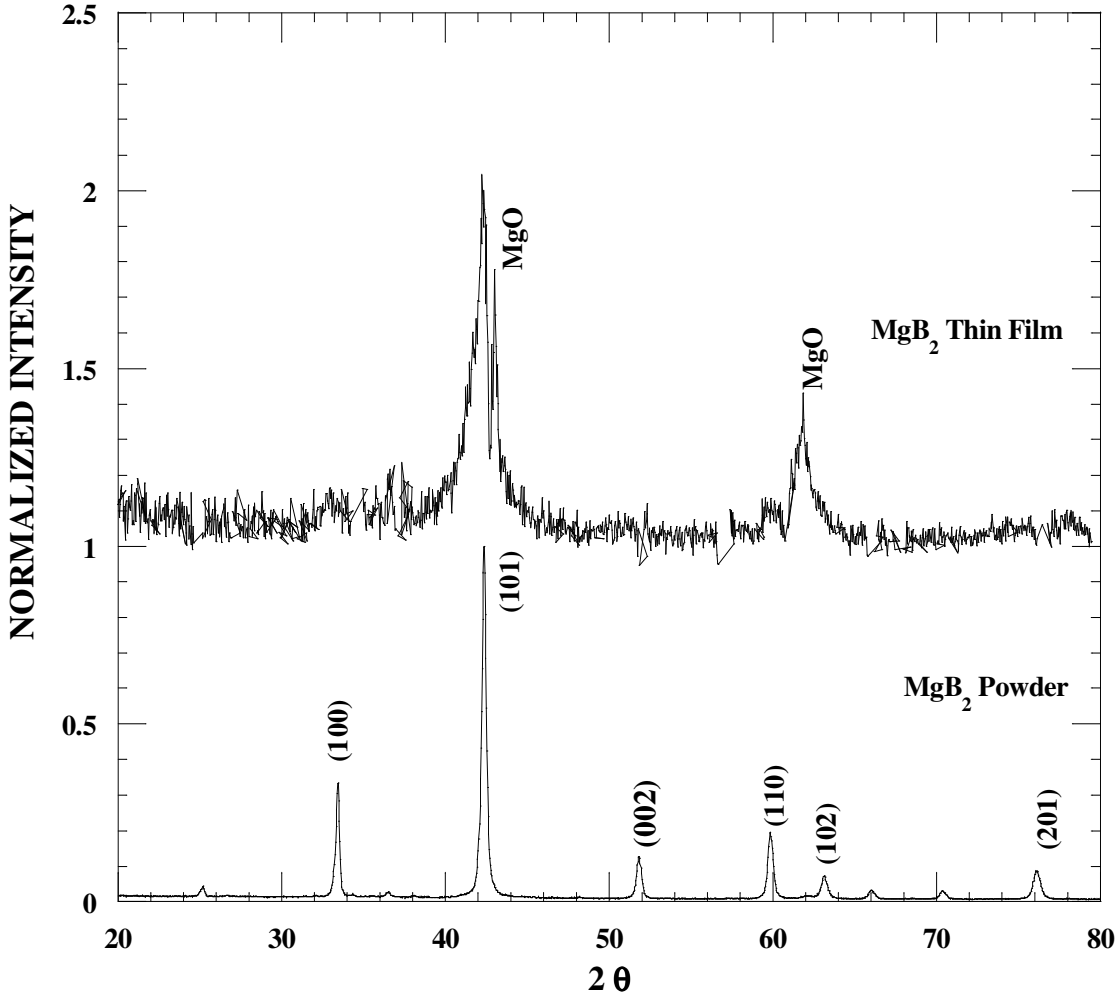

Figure 4.7. XRD Patterns of 650 ^{o}C–30 min. annealed MgB_2 thin films- MgB_2 powder

4.2. SEM and EDX Results

To investigate the microstructure of the grown films and the surface morphology of the grown films, Scanning Electron Microscopy (SEM) was used. All the surface images were taken from grown films on Al_2O_3 polycrystal substrate. To measure the thickness of the MgB_2 thin films, cross section SEM images were taken from films on Al_2O_3 polycrystal substrate and $LaAlO_3$ single crystal substrate. All the SEM images were taken in same magnification values to make better comparison.

Figure 4.8 shows the SEM image of Al_2O_3 substrate and the Figure 4.9 shows the SEM image of as-grown film on Al_2O_3 polycrystal substrate. We used the Al_2O_3 polycrystal substrate SEM image to investigate surface of the grown films. As seen from the Figure 4.8, the Al_2O_3 polycrystal substrate has several grains in different size. After deposition, film is covered the surface of the substrate shown at figure 4.9. At the as-grown sample image, Al_2O_3 grains can be still observed but film can be easily observed on the substrate. It can be said that film preferred to grow on grains of the Al_2O_3 polycrystal substrate.

Figure 4.10 to Figure 4.13 show the SEM images of the films after an ex-situ annealing process. These SEM images show the effects of ex-situ annealing process on as-grown film surface morphology. When annealed films images are compared to as-grown film image, changing of the sample surface morphology can be observed

The 625 ^{o}C-20 min. annealed sample, the grains of the substrate can be hardly observed. The grown films after an ex-situ process are denser than as-grown films. Based on the XRD results, it can be thought that the crsytalinty starts to occur. After increasing the annealing temperature from 625^{o}C to 650^{o}C for 20 min annealed sample, the grains of the substrate start to be observed. In 650 ^{o}C-20 min. sample some particles occurs in white color. We observed that these particles are MgO, after EDX studies on these small regions. In the Figure 4.12 and Figure 4.13, films annealed at 30 min. samples are shown. The grains of the substrate can be hardly observed after ex-situ annealing process.

According to all SEM images, it can be said that films grown on grain of the substrate and annealed films are denser than the as-grown films.

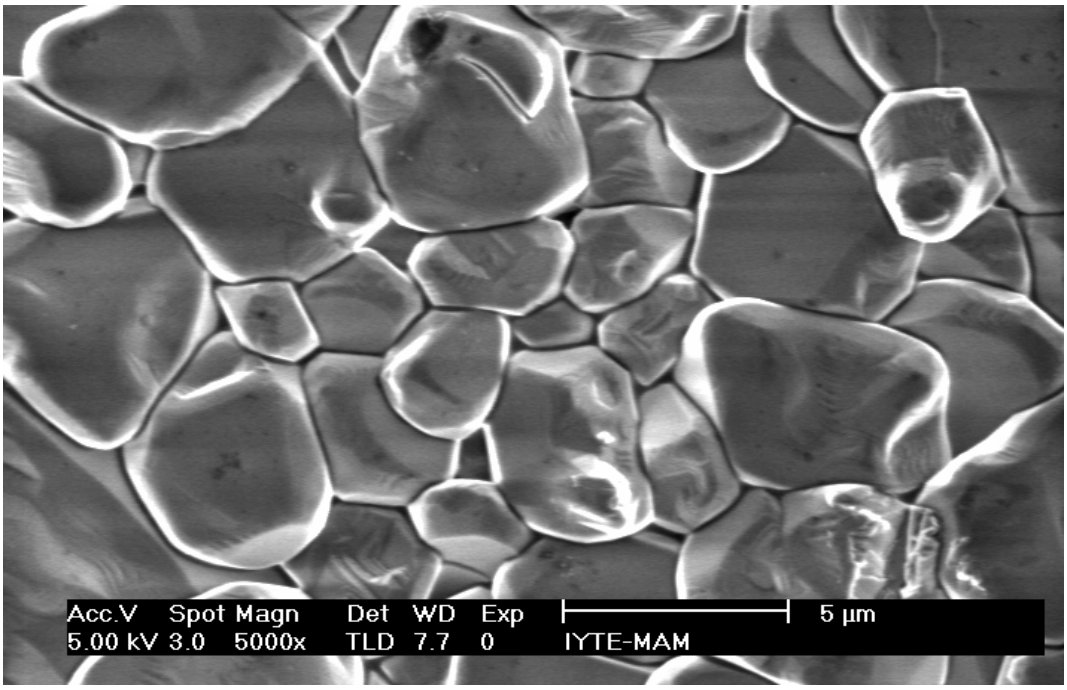

Figure 4.8. SEM image of Al_2O_3 polycrystal substrate

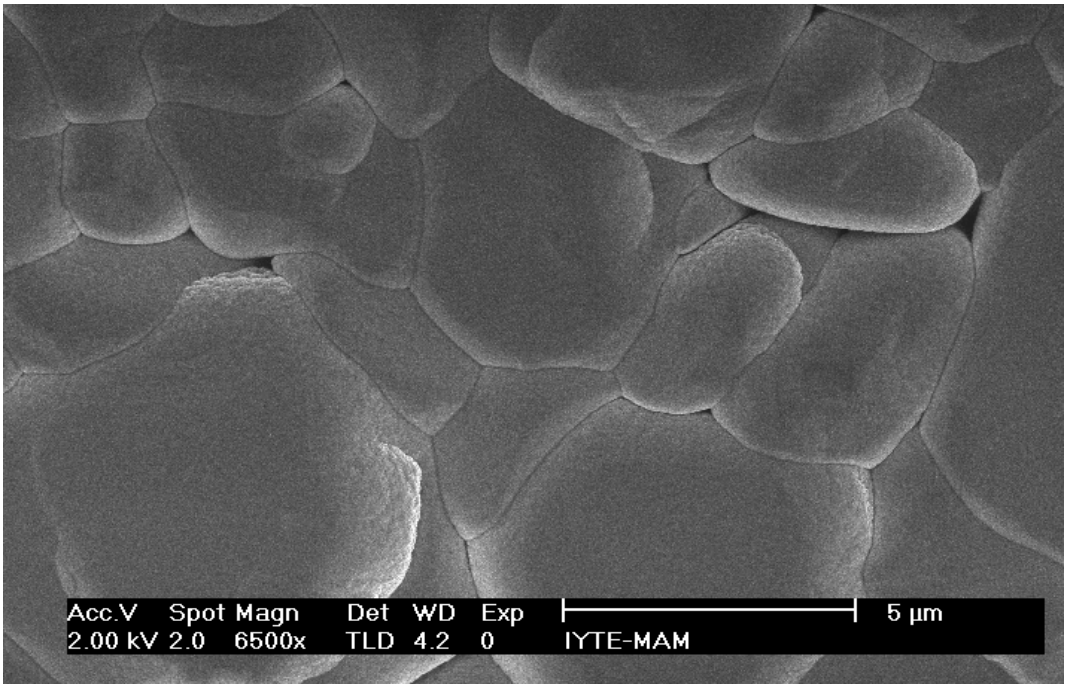

Figure 4.9. SEM image of as-grown film on Al_2O_3 polycrystal substrate

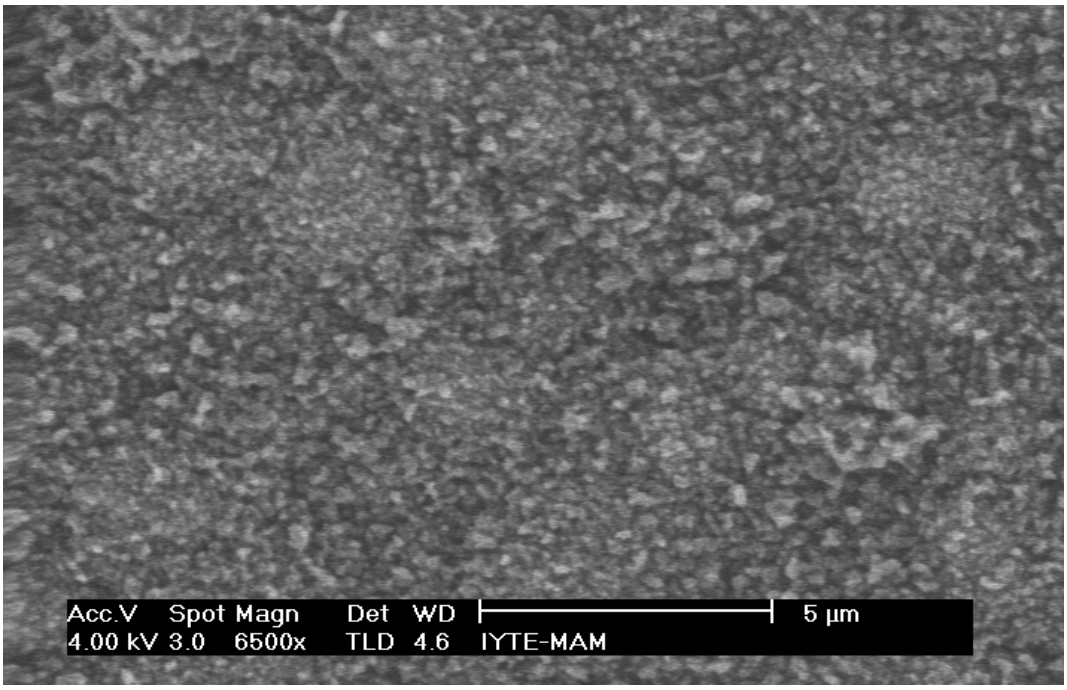

Figure 4.10. SEM image of 625 ^{o}C-20 min. annealed MgB_2 film on Al_2O_3 Substrate

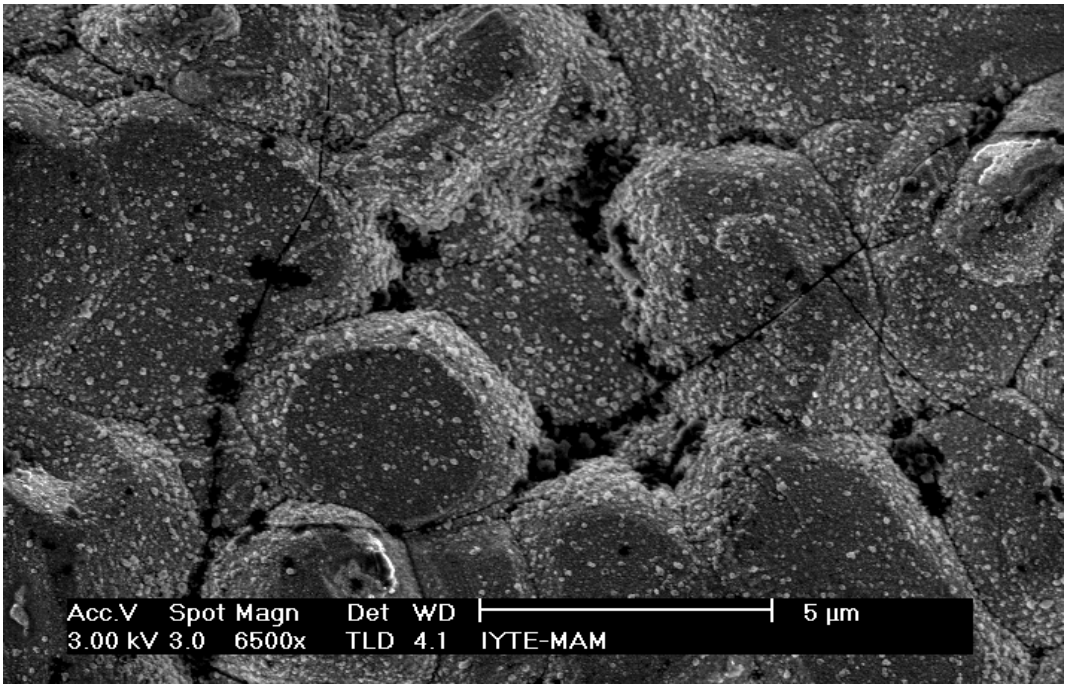

Figure 4.11. SEM image of 650 ^{o}C-20 min. Anneal MgB_2 film on Al_2O_3 Substrate

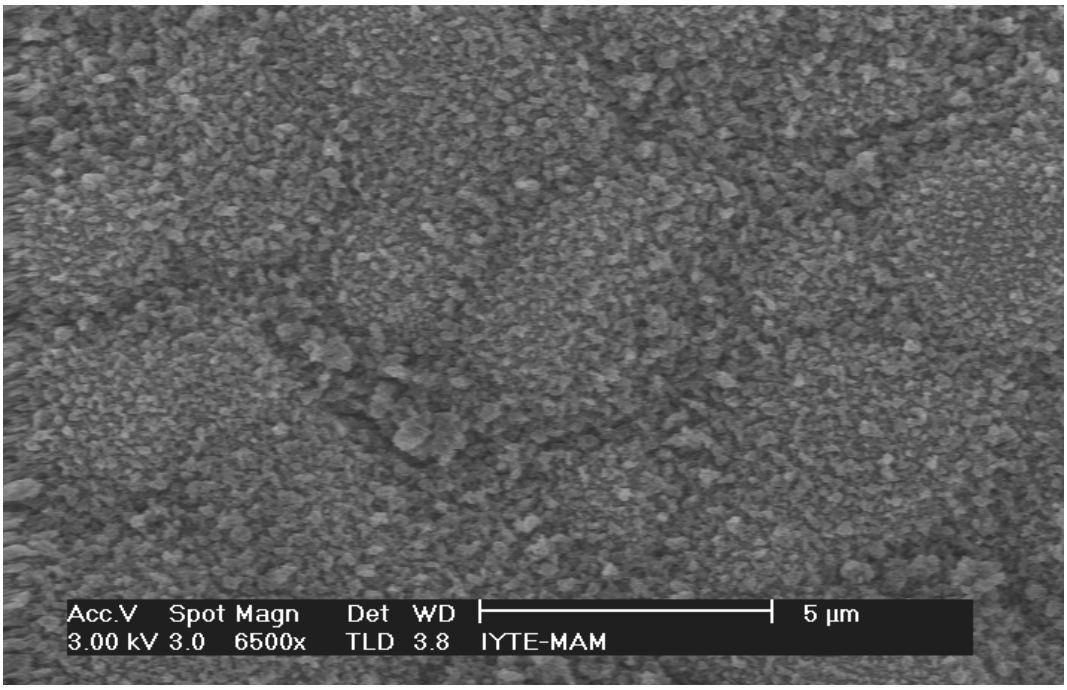

Figure 4.12. SEM image of 625 ^{o}C-30 min. Anneal MgB_2 film on Al_2O_3 Substrate

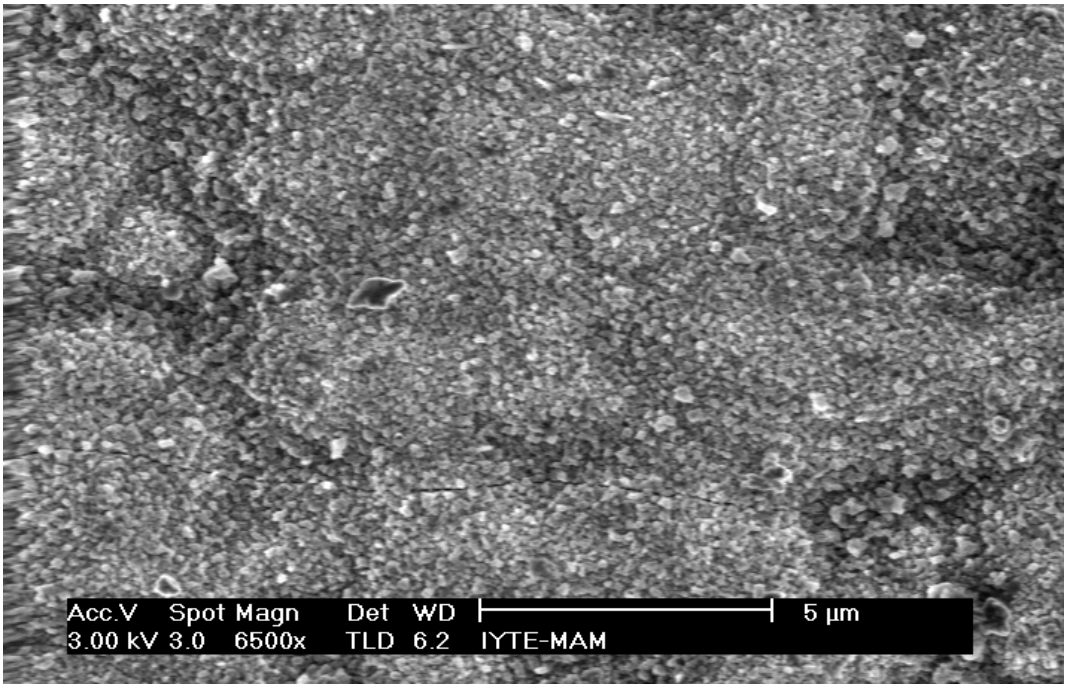

Figure 4.13. SEM image of 650 ^{o}C-30 min. Anneal MgB_2 film on Al_2O_3 Substrate

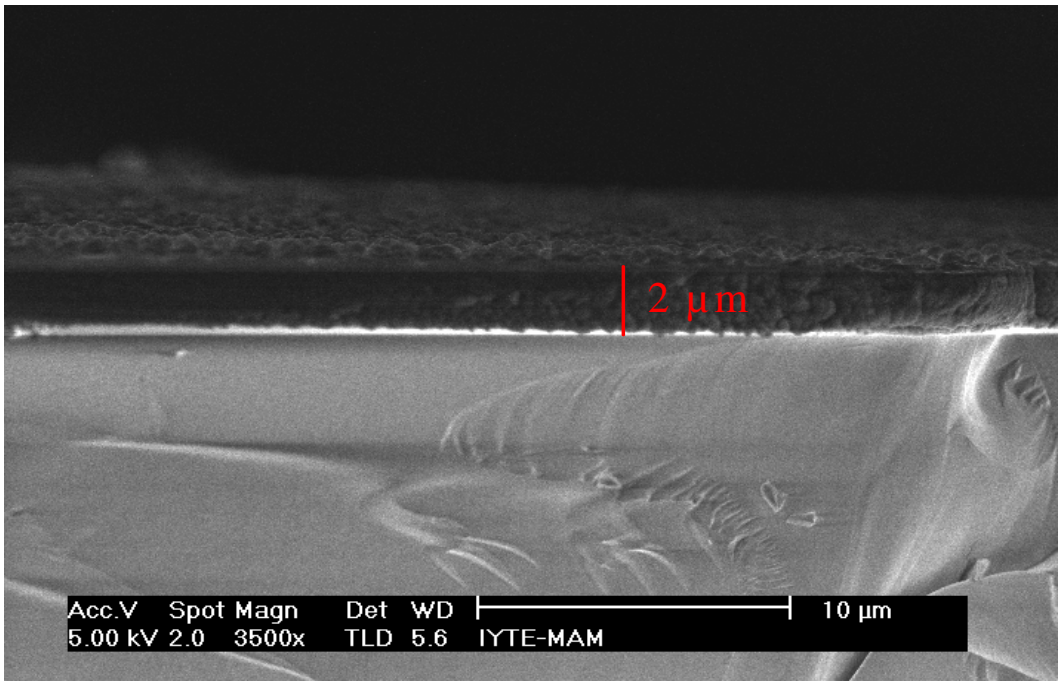

Figure 4.14. Cross section SEM image of MgB_2 film on $LaAlO_3$ Substrate

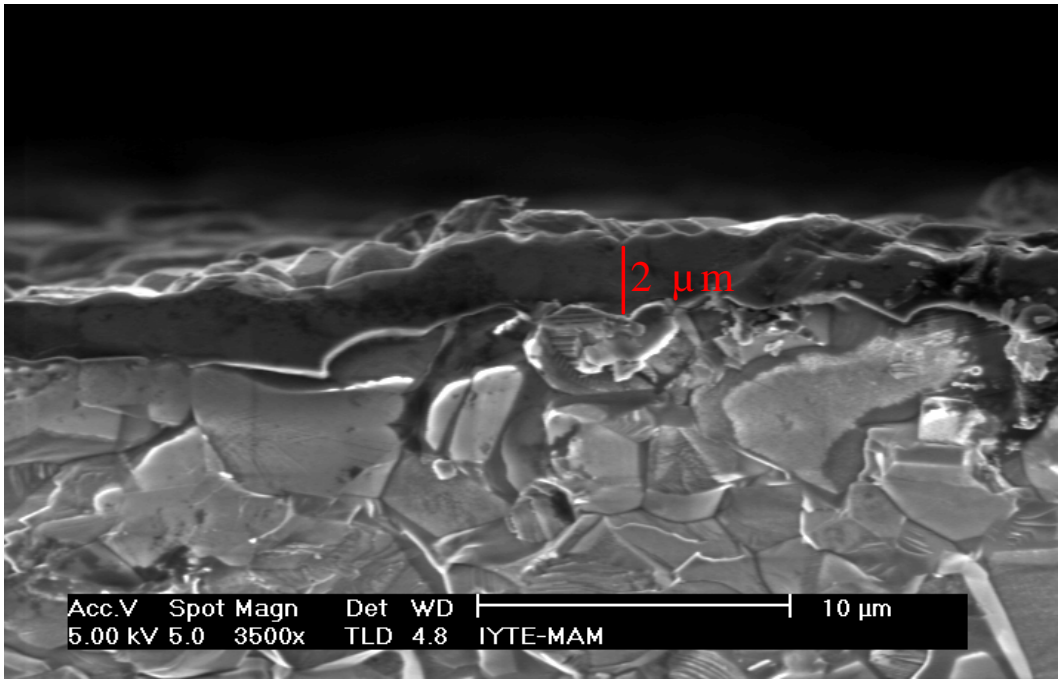

Figure 4.15. Cross section SEM image of MgB_2 film on Al_2O_3 Substrate

To measure the thickness of the films, SEM cross section image of the films were used. The Figure 4.14 and 4.15 shows the cross section of the MgB_2 thin films grown on 2 different substrates, $LaAlO_3$ (001) single crystal and Al_2O_3 polycrystal.

The measured thicknesses of films are about ~2μm. During the deposition we used a constant deposition time and the distance between target and substrate was the same in all experiments. Therefore, all deposited films have same thickness.

On the other hand, film grown on $LaAlO_3$ (001) substrate is smooth as seen in Figure 4.14, but films was grown on Al_2O_3 substrate roughly as seen in Figure 4.15 because of the rough surface of the Al_2O_3 polycrystal substrate

Table 4.1. EDX Results of 20 min. Anneal MgB_2 films

Material	As-Grown	625 ^oC	650 ^oC
%Mg	33.75	32.60	43.45
%B	56.09	37.70	33.40
%O	10.16	29.70	23.10

Table 4.2. EDX Results of 30 min. Anneal MgB_2 films

Material	As-Grown	625 ^oC	650 ^oC
%Mg	33.75	40.70	50.19
%B	56.09	25.83	15.38
%O	10.16	29.46	34.42

Tables 4.1 and 4.2 show the Energy Dispersive X-Ray (EDX) results of as-grown and annealed MgB_2 thin films. EDX analyses were done to obtain the chemical content of the films. In order to collect the best data from the surface, same electron energies were used in all experiments. The EDX results show that the oxygen content increased in all annealed films, when compared with as-grown films. The EDX results show any stoichometry of Mg_xB_y. The oxygen source can be porosity of the target, impurity of the MgB_2 powders and impurity of Ar gas mentioned in XRD results.

4.3. Low Temperature Electrical Properties

Since the simplest explanation of the superconductivity is the loss of resistivity below a certain temperature, the transition temperature (T_c), the determination of this temperature is very important. There are mainly two methods for determining transition temperature; the measurements on the temperature dependence of sample resistance and temperature dependence of magnetization. In this study; only temperature dependence of sample resistance was study to determine transition temperature of the films. In order to determine the T_c, traditional four-point method was used.

To calculate the parameters of temperature dependence of resistance measurements, dR/dT (derivative of the resistance dependence of temperature) were taken. Mathematically, a superconducting transition graph can be described as a step function. Therefore, derivative of this graph give us a peak at the T_c value of the graph. From the dR/dT - Temperature graphs, T_c^{onset}, T_c^{zero}, T_c^{mid}, ΔT values can be calculated. On the point of physics the temperature, which the transition begins is important, called onset critical temperature. However, on the point of engineering view the temperature that zero resistivty is very important, called zero critical temperature. These parameters can describe the superconducting quality of the materials. At dR/dT–Temperature graph, the maximum peak point show the middle transition temperature point, T_c^{mid}. 10% of maximum peak values give the 90% and 10% values of the onset transition temperature. ΔT value can be determined by differences of these values. Figure 4.17 and Figure 4.16 show the example of dR/dT-Temeprature graph and temperature dependence resistance graph of 625 ^oC-20 min. annealed sample.

In addition to this; to determine the upper critical magnetic field (H_{c2}) values of the MgB_2 films, four-point measurements were done under various magnetic field values; 0T, 3T and 6T. Magnetic field applied perpendicular to the sample surface. After these measurements, to fit the experimental points, a graph programs (k-graph) was used for prediction of the upper critical magnetic field.

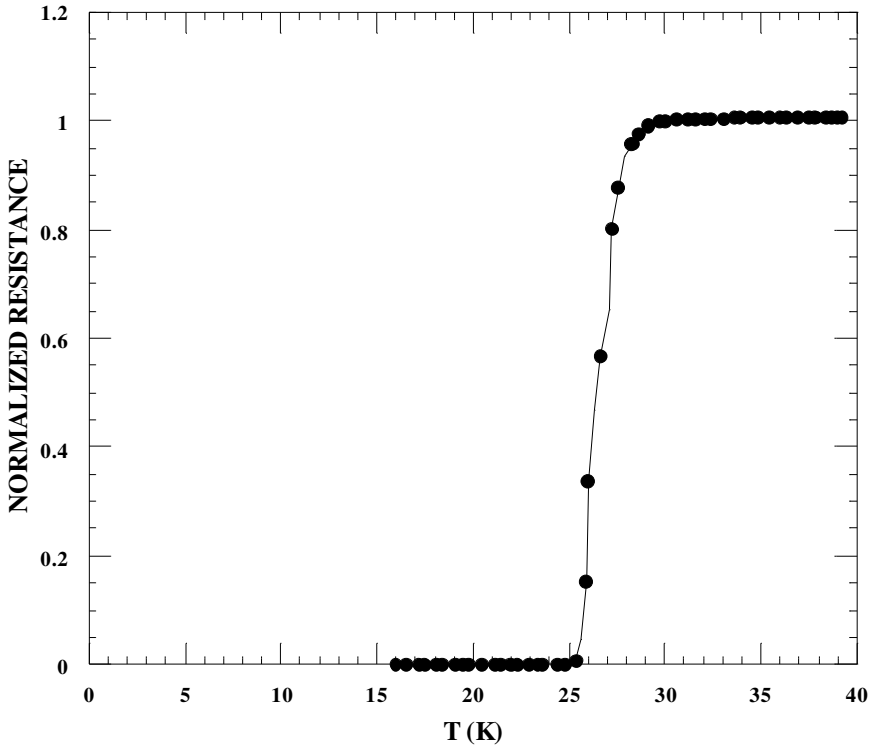

Figure 4.16. Resistance-Temperature results of 625 ^{o}C-20 min. annealed sample

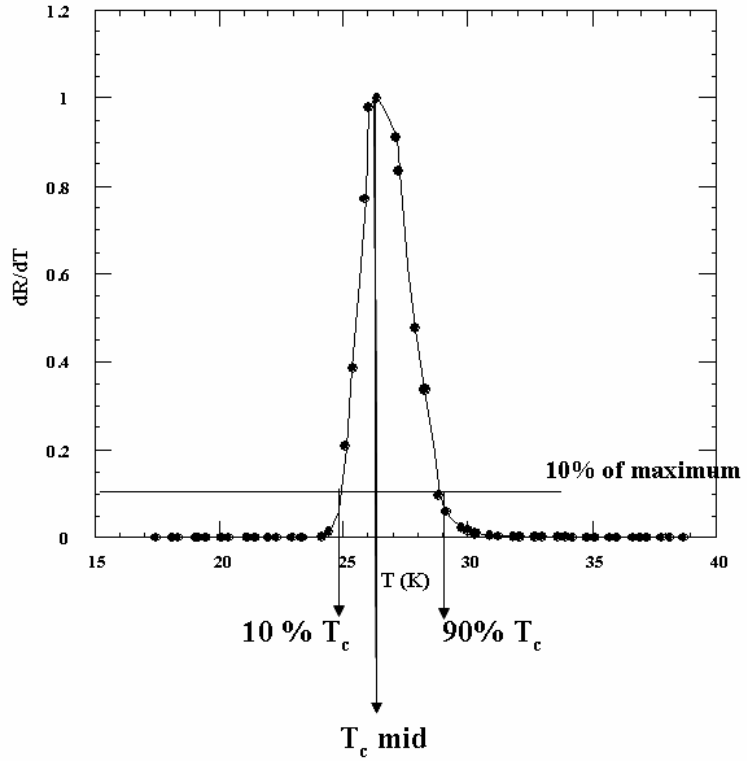

Figure 4.17. dR/dT-Temperature graph of 625 ^{o}C-20 min. annealed sample

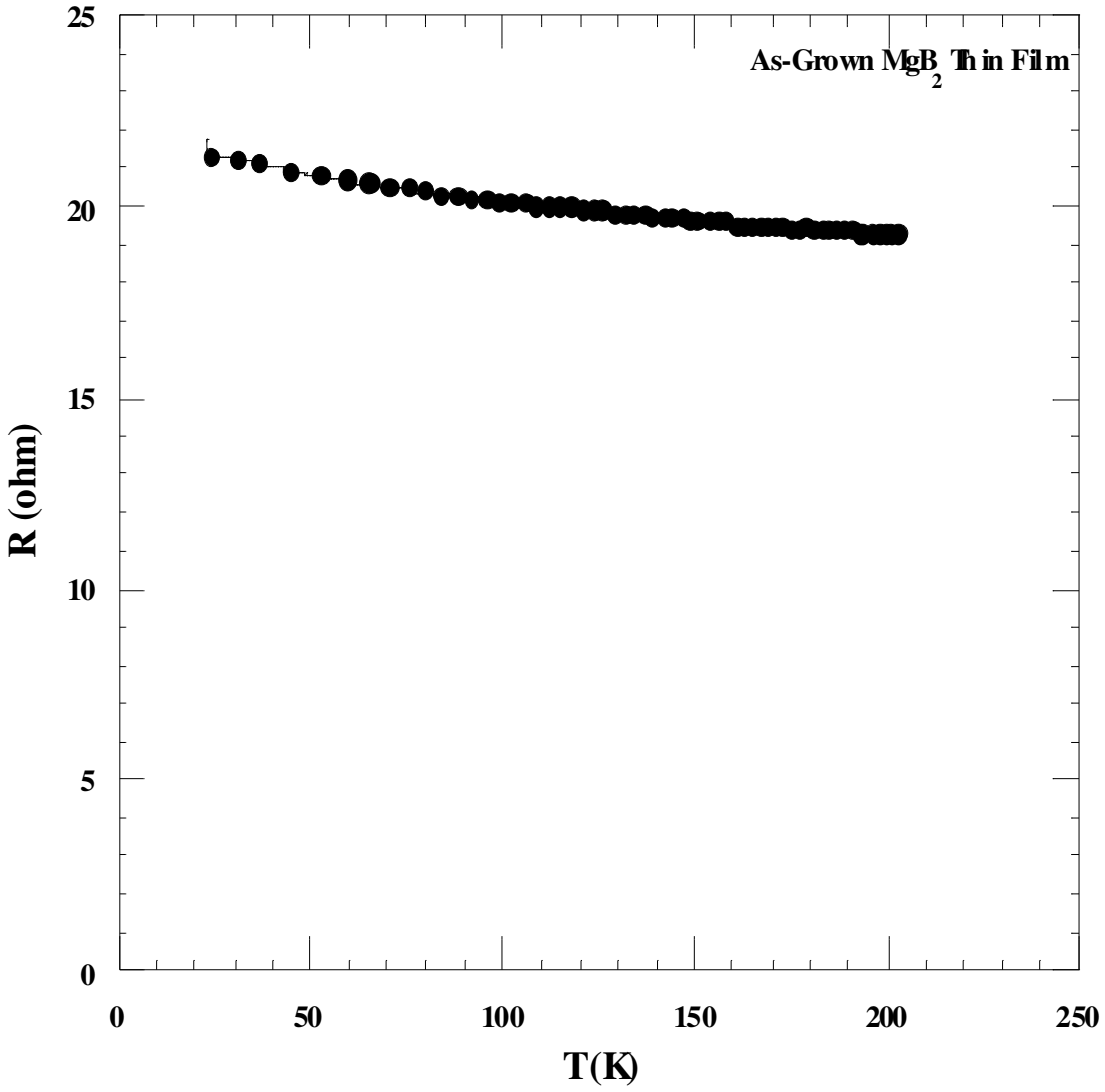

Figure 4.18. Resistance-Temperature results of as-grown films

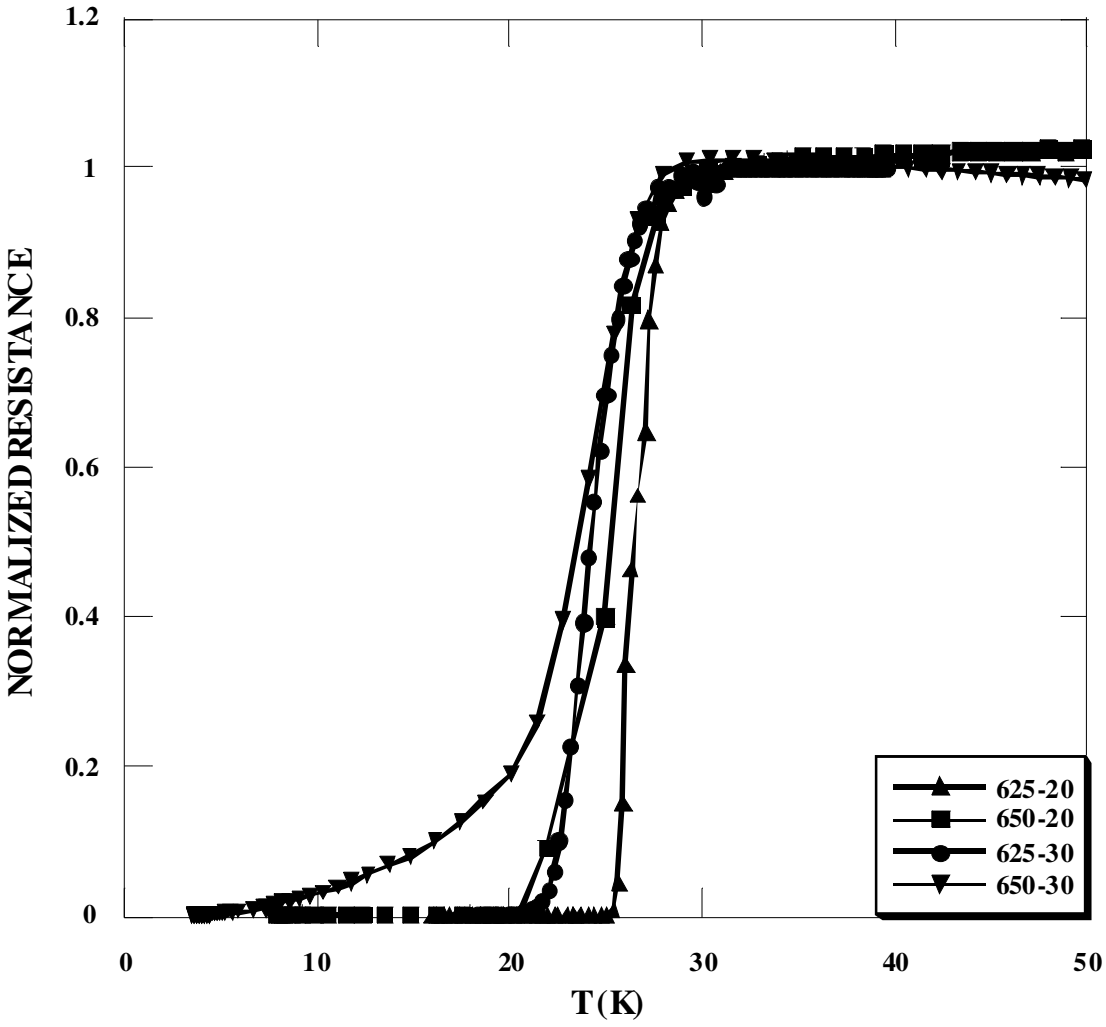

Figure 4.19. Resistance-Temperature results of annealed films.

Table 4.3. The T_c, ΔT, T_c^{Onset}, T_c^{Zero} , T_c^{Mid} , T_c 90%, T_c 10% values of the MgB_2 thin films

Temperature/Time	T_c 90%	T_c 10%	T_c^{Onset}	T_c^{Zero}	ΔT	T_c^{Mid}
625-20	28.64	24.81	30.04	25.40	3.83	26.31
650-20	28.83	21.16	29.03	20.41	7,67	26.32
625-30	27.08	21.59	27.47	20.08	5.49	24.09
650-30	29.02	15.57	30.47	9.08	13.45	25.39

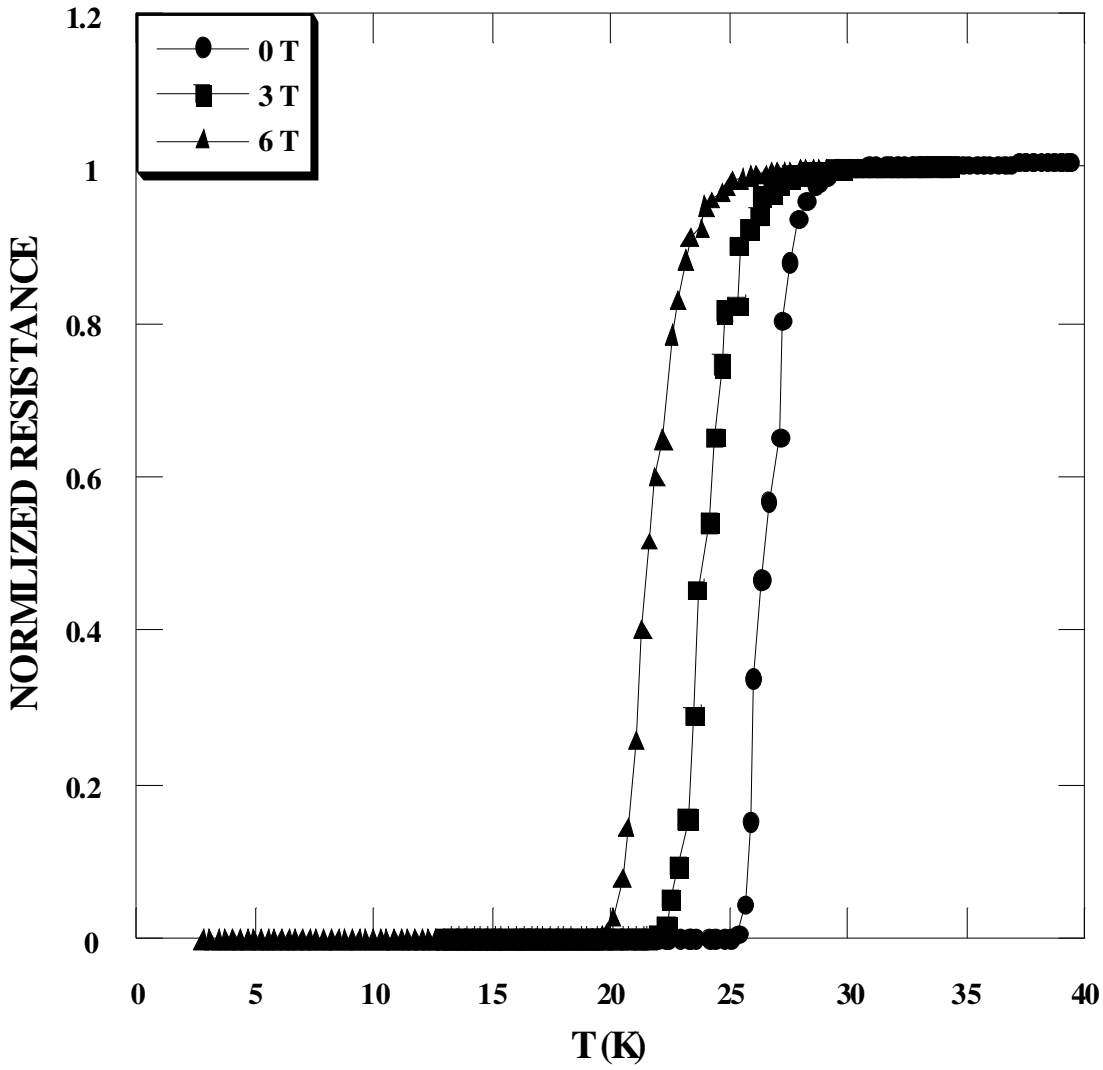

Figure 4.20. Resistance-Temperature results of 625 ^{o}C-20 min. annealed sample under various magnetic fields

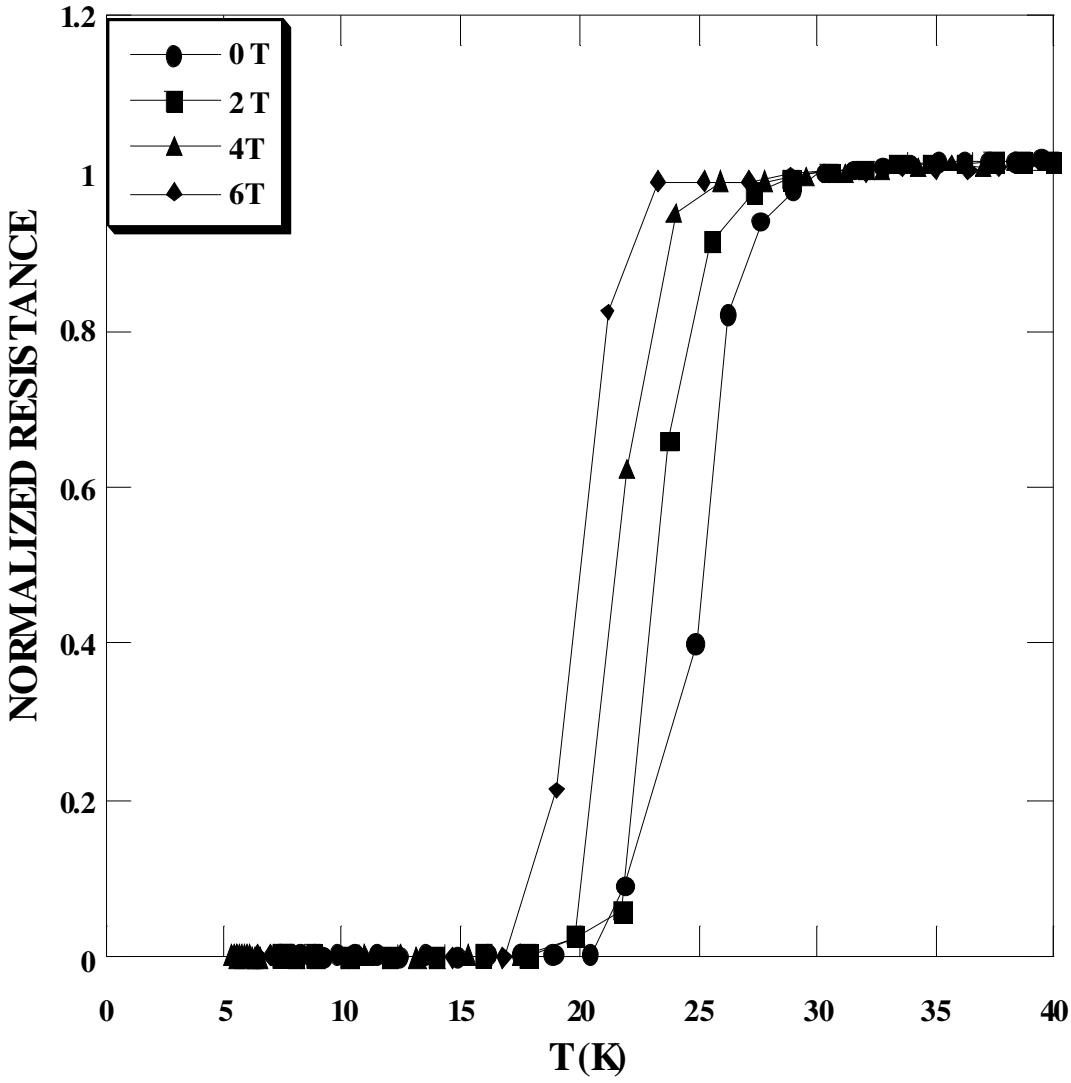

Figure 4.21. Resistance-Temperature results of 650 ^{o}C-20 min. annealed sample under various magnetic fields

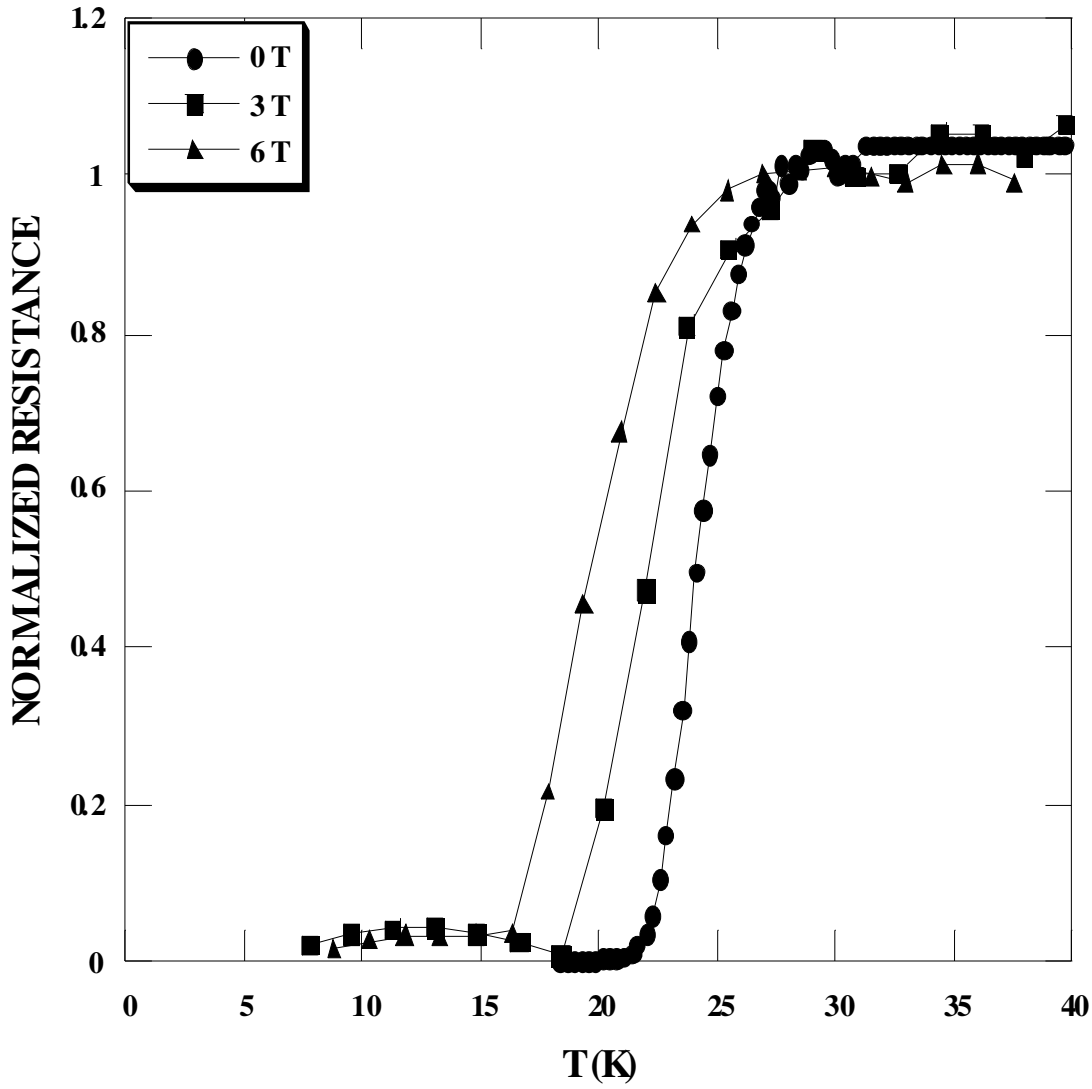

Figure 4.22. Resistance-Temperature results of 625 ^{o}C-30 min. annealed sample under various magnetic field

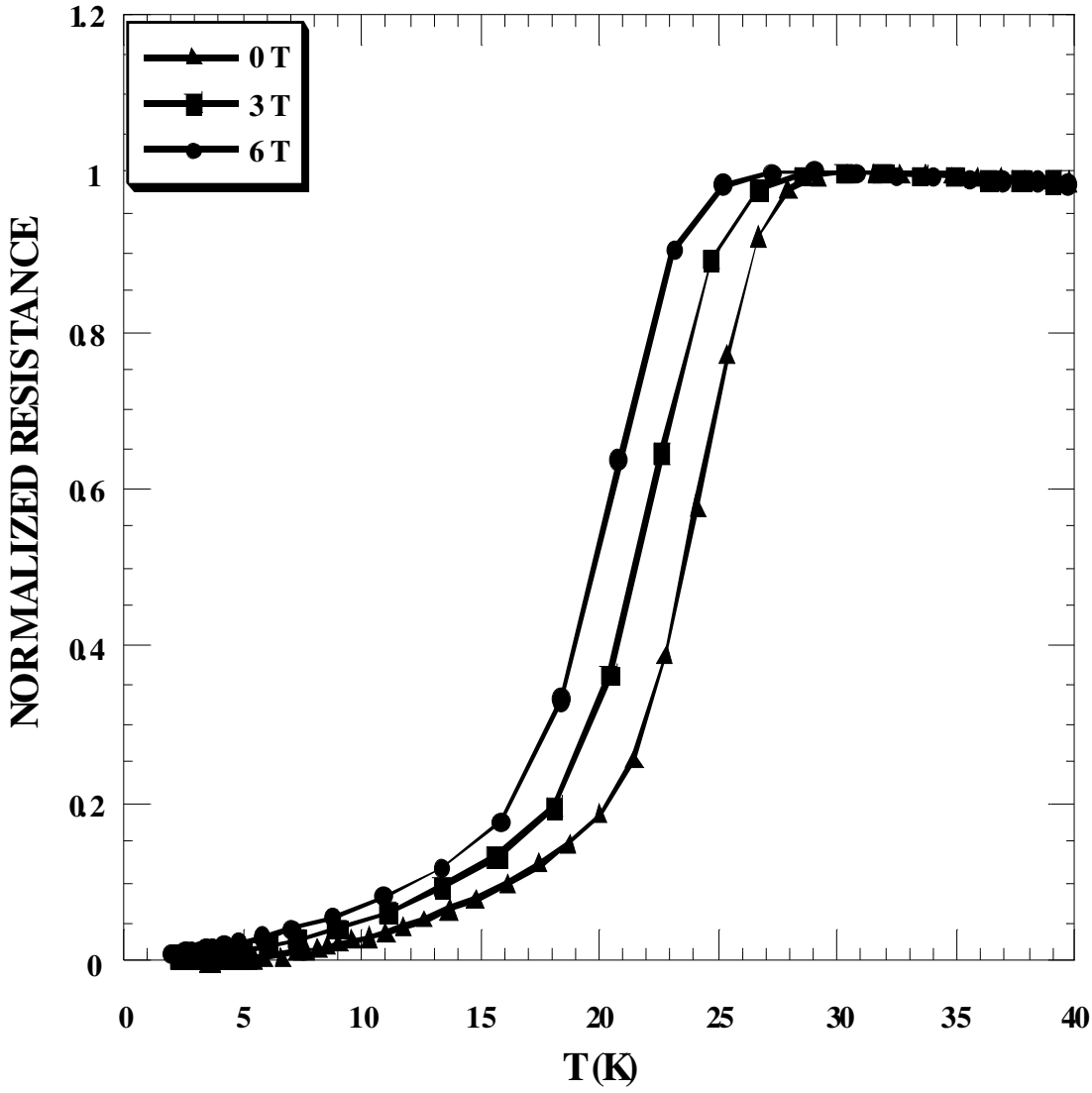

Figure 4.23. Resistance-Temperature results of 650 ^{o}C-30 min. annealed sample under various magnetic fields

Figure 4.18 shows temperature dependence resistance measurement of the as-grown film. This graph was plotted from room temperature (300 K) to low temperature (15 K). Mainly, as-grown film didn't show a superconducting transition. In addition to this, XRD patterns of the as-grown films show that any crystalline was observed. As-grown films have totally amorphous phase. For this situation; it can be thought that MgB_2 can be decomposed during the deposition process. On the other hand, as-grown films show a semiconductor behavior in temperature dependence resistance measurement.

Temperature dependence resistance graphs for all annealed films were shown in Figure 4.19. The resistances values of all films were normalized to 30 K values of them. Table 4.3 shows the calculated values, T_c 90%, T_c 10%, T_c^{Onset}, T_c^{Zero}, ΔT, T_c^{Mid}, of the annealed films. These values were calculated by using dR/dT versus T graphs. After ex-situ process, all films show the superconducting transition in different qualities. The best T_c^{Onset} value was obtained from 625 ^oC-20 min. sample at ~30 K. The T_c^{Mid} temperature of this film is at 26.31 K. It has best ΔT values, which is 3.8 K. According the previous study by using magnetron sputtering (Mancini et al 2003, Ermolov et al 2001, Mori et al 2004, Ohkubo and Akinaga 2004, Akinaga et al. 2003,Vaglia et al. 2002) generally T_c values was lower than the ~30 K. It shows that the difficulties of MgB_2 thin film preparation by using magnetron sputtering system.

Increasing annealing temperature decrease the ΔT values of the annealed samples. In high temperature annealing process (at 650 ^oC) MgB_2 films annealed for 20 min. or 30 min show large broaden transition when they compare with the low temperature annealed samples (at 625 ^oC). Additionally, increasing annealing times decrease the superconducting properties of the films. All annealed films show nearly same T_c temperature, but ΔT values are very different from each other. This changing in the ΔT can be dependent of the impurity of the films, because this value reaches to ~16 K at 650 ^oC-30 min. annealed sample. In this sample an impurity can be easily observed at low temperature after transition because of showing resistance.

For all samples, the resistivity values are measured. They are shown in Table 4.4. Measured values of resistivity shows the high resistivity, when we compare the MgB_2 resistivity value even at room temperature (4.5 $\mu\Omega$cm at 300 K) (Rowell 2003). In 2003 Rowel reviewed the resistivity behaviors of MgB_2 and their temperature dependences for thin films, single crystals and polycrystalline samples.

Table 4.4. Resistivity values of the MgB_2 films at 30 K

Samples	ρ (mΩ.cm)
As-Grown Film	4.30
625 ^{o}C-20 min. annealed	1.40
650 ^{o}C-20 min. annealed	0.28
625 ^{o}C-30 min. annealed	0.60
650 ^{o}C-30 min. annealed	83.00

The sample annealed at 650 ^{o}C-20 min sample show the best resistivity around transition temperature. Increasing annealing temperature decreases the resistivity of the sample. It show that ex-situ anneal process develop the resistivity of the sample. On the other hand, the highest value of resistivity values can be observed in the 650 ^{0}C-30 min. sample. We observed a large broaden transition; ΔT is around 17 K at this sample. This situation can be explained by the loss of Mg and oxidation of the Mg during the deposition and annealing process. The figures 4.20 to 4.23 show the temperature dependence resistance characteristic of the annealed films under various magnetic fields. All magnetic fields were performed perpendicular to the film surfaces and magnetic field was applied during the cooling processes called field cooling (FC). The main observation from the figures is that increasing the applied magnetic field decreases the T_c of the films. It is the characteristic property of superconductor materials. To observe the upper critical magnetic field value of prepared films, all T_c values of the films were calculated under various magnetic fields. The founded values were marked in a magnetic filed versus temperature graphic. The best line was plotted according these data. The interception of the line at magnetic field axis was accepted maximum value of upper critical magnetic field. Then, this value was started to examine in equation 4.1. MgB_2 is the low temperature superconductor material. Therefore the equation 4.1 was used.

$$B_c (T)= B_c(0) [1- (T/T_c)^2] \quad (4.1)$$

To plot best graphic related to equation 4.1, a graphic program (k-graph) was used. Figures 4.24 and 4.25 show the best fitting graph by using experimental data. Our data shows that predicted upper critical magnetic field values, $H_{c2}(0)$, are ~17 Tesla for 20 min. annealing samples and ~19 Tesla for 30 min. samples. These values are good for ~ 25 K T_c temperature samples. (Patnaik et al 2001, Xu et al 2001, Buzea and Yamashita 2001).

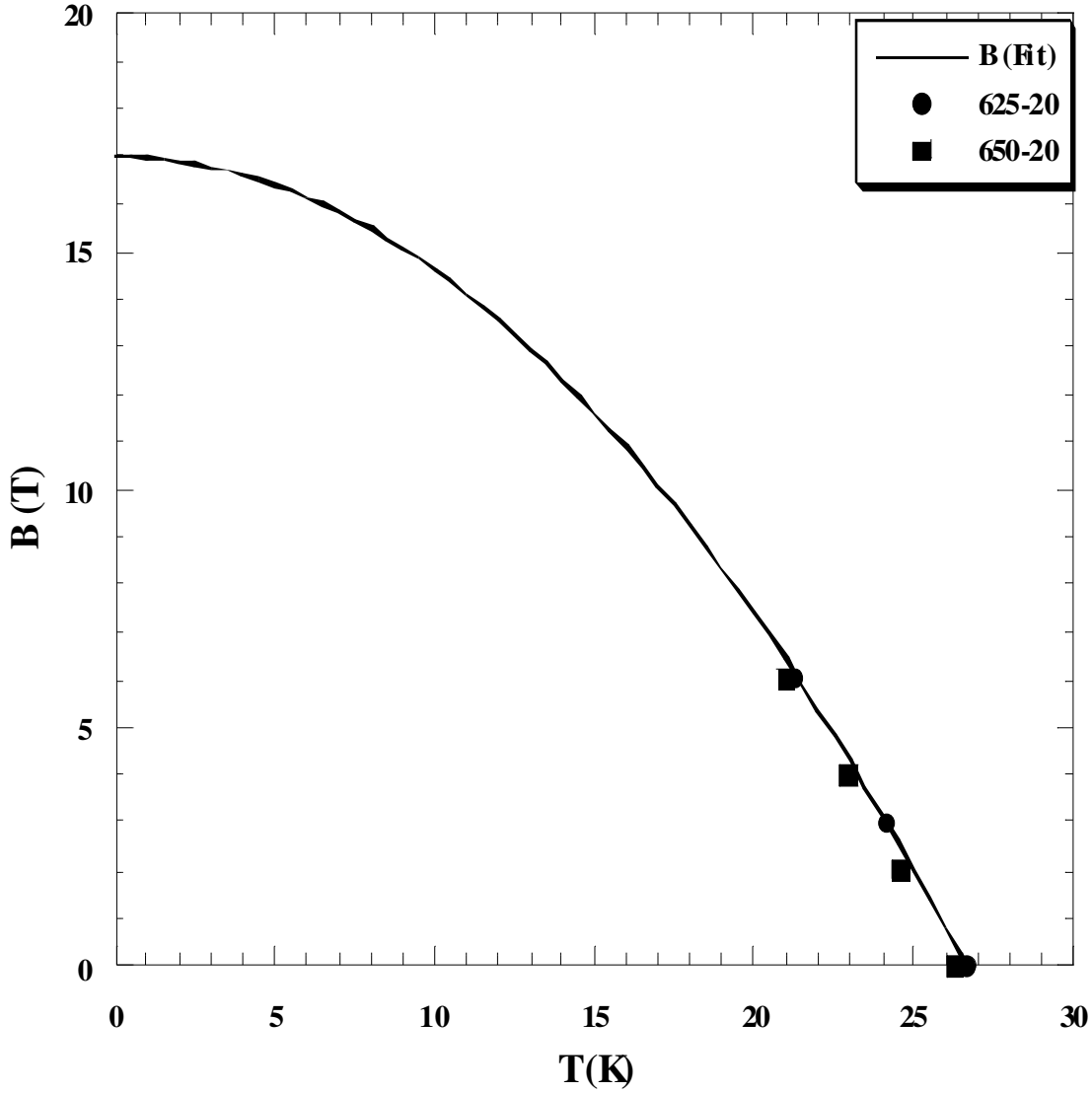

Figure 4.24. Magnetic Field – Temperature 20 min. annealed samples

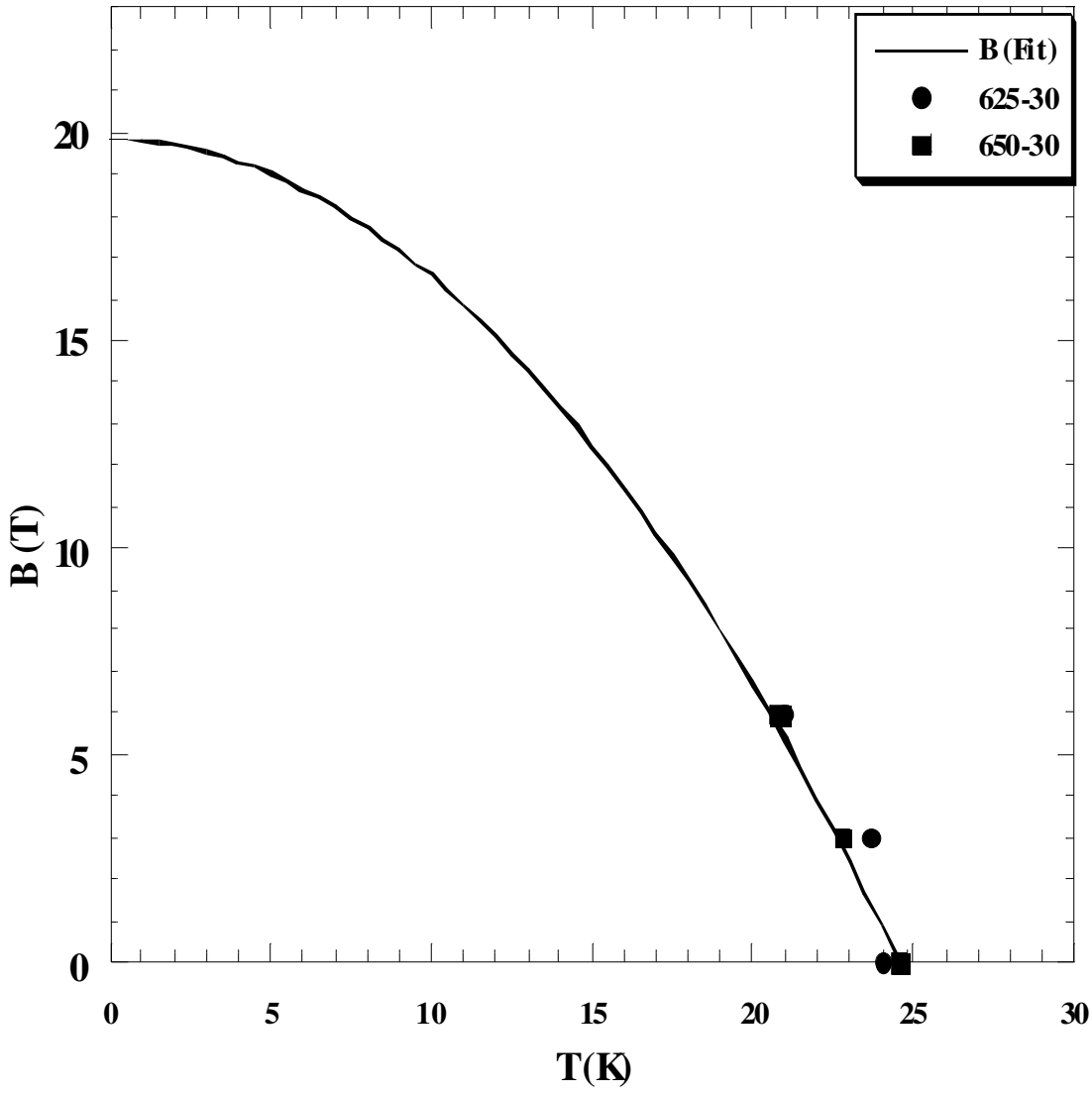

Figure 4.25. Magnetic Field – Temperature 30 min. annealed samples.

CHAPTER 5

CONCLUSIONS

The discovery of superconductivity at 39 K in the intermetalic compound MgB_2 in 2001 raised the great interest for the both science and technology applications. It has the highest T_c value among the intermetalic compounds. MgB_2 has many properties make it very attractive for superconducting applications, especially electronic applications; these are large coherence length, high critical current density (J_c), high critical magnetic field (B_c). MgB_2 thin film technology was developed by using these good superconducting properties to produce high quality superconducting electronic circuits. Several methods were developed for growth of high quality MgB_2 thin films mentioned in chapter 2.

In this study, we tried to deposit MgB_2 thin films by using a high vacuum magnetron sputtering system. Firstly, a MgB_2/Mg composite 2 inches magnetron sputtering target was produced with a hot pressing technique using commercially available MgB_2 and Mg powder mixing in air. MgB_2 thin films were grown a Al_2O_3 polycrystal substrate and $LaAlO_3$ (001) single crystal substrate. The second step was carried out to perform MgB_2 thin film. This was ex-situ annealing procedure. Various annealing temperatures, 625 ^oC and 650 ^oC, and various annealing times, 20 min. and 30 min., were examined to increase the quality of as-grown MgB_2 thin films. After thin film growth steps, some characterization techniques were applied to obtain structural properties and low temperature electrical characteristics for prepared MgB_2 thin films. Our aims of that were to grow MgB2 thin films by using a magnetron sputtering system and to develop the ex-situ annealing conditions for increasing the quality of MgB_2 superconductor thin films.

To better make compression, all XRD data were taken in same 2θ region. XRD results showed that our as-grown films have not any crystal peak at the scanned region. As-grown films have totally amorphous structure. After ex-situ process, all MgB_2 thin films grown on Al_2O_3 substrate show crystalinity. The main phase of annealed films are MgB_2 (101) at $2\theta = 42.5$. After ex-situ process at different conditions, all samples show this main peak of MgB_2 in different quality that means peak width and sharpness. When compared the 20 min. annealed samples, peak of (101) the MgB_2 thin films annealed at

650 ^{o}C become sharper than annealed at 625 ^{o}C one. At the 30 min. annealed sample, increasing temperature develop this main peak of the MgB_2 thin film. On the other hand, some poor crystalline peak related to MgB_2 phase occurred in 625 ^{0}C annealed sample. This showed that increasing annealing temperature decreases the crystal quality of MgB_2 thin films. In addition to these observations, the second phase related to MgO peaks occurred in all annealed samples. Every annealed sample have a poor MgO peak around $2\theta=61,6^{o}$ position. Especially, increasing annealing temperature increase the new MgO peak $2\theta = 43^{o}$. For 30 min. annealed samples, this MgO peak is more detectable at 650 ^{0}C than at 625 ^{o}C. The reason of the MgO phase can be related to impurity of the starting materials, those are MgB_2 and Mg powders. We prepared the sputtering target at atmosphere under hot pressing technique. This is lead to oxidation of Mg because of sensitivity of it to oxidation. In addition to this we used Ar gas (purity 99.99%) during the ex-situ annealing process. This can be another reason for oxidation.

SEM results show the surface morphology of the films grown on Al_2O_3 polycrystal substrate. As-grown film can be observed when it was compared with the substrate image. After ex-situ annealing process, grains of the substrate is not easily observed. Films prefer to grow on Al_2O_3 polycrysatal substrate grains. Cross section images of the film grown on Al_2O_3 polycrystal substrate and $LaAlO_3$ single crystal substrate showed the thickness of the films. Prepared films have 2 μm thicknesses. EDX data are taken to determine the chemical content of the films. They show ex-situ annealing process increase the oxygen amount of the samples. These are related to annealing conditions and starting materials impurity.

Temperature dependence resistance measurements were performed by traditional four point method. Measurements showed that as-grown films without ex-situ annealing have not superconducting transition. It can be thought that MgB_2 could be decomposed during the deposition process. Then, high resistance of as-grown samples shows the lack of Mg. To prevent the loss of Mg, excess Mg was added to MgB_2 powder as the target was prepared. In addition to this XRD results mentioned above show that as-grown films have amorphous phase. These reasons can be explain why the as-grown films don't show any superconducting transition. After ex-situ annealing process, all films show a superconducting transition at different transition temperature. The best transition was observed at 625 ^{o}C-20 min. annealed sample. It has a high T_c^{onset} value at ~30 K when we compared with literature about MgB_2 thin film prepared by magnetron sputtering system. This sample has best broaden transition

temperature value, ΔT= 3.83 K. Generally T_c^{Mid} of the annealed sample are same those are 24 K–26 K. The differences between the samples occur at ΔT values. It can be observed that increasing annealing temperature and annealing times increase the ΔT values of the samples. This value is ~14 K for the 650 ^oC-30 min. sample. On the other hand, measured resistivity of the sample at 30 K is higher than the MgB_2 resistivity generally. This high resistance is a result of loss of Mg and MgO phase in our samples. The temperature dependence resistance measurements that are made under various magnetic fields gives us magnetic properties of the prepared sample after ex-situ annealing process. These measurements are providing to make a prediction about upper critical field value of the films. After best fitting of data, upper critical magnetic fields are found about 17 T and 19 T for all films. These values are well compared literature for this transition temperature values.

Finally, we achieved to product a MgB_2 target for a magnetron sputtering system. To deposit superconducting MgB_2 thin film, a high vacuum magnetron sputtering system was used. To enhance the superconducting properties of the films and to increase the crystal quality of the prepared films an ex-situ annealing process was performed. Ex-situ annealing process develops the structure and electrical properties of the MgB_2 thin films.

REFERENCES

Ahn, J.R., Lee, S.G., Hwang, Y., Sung, G. Y., Kim, D. K. 2003. "Fabrication of MgB_2 thin film by rf magnetron sputtering", *Physica C.* Vol. 388-389, p. 127.

Akinaga, M. 2003. "Synthesis of as-grown superconducting MgB_2 thin films by sputtering method", *Cyrogenics*. Vol. 43, p. 567.

Bardeen, J., Cooper, L. N., Schrieffer, J. R. 1957. "Microscopic Theory of Superconductivity", *Phys. Rev*. Vol. 106, No. 1, p. 162.

Bednorz, J.G. and Müller, K.A. 1986. "Possible highT_c superconductivity in the Ba–La–Cu–O system", *Zeitschrift für Physik B Condensed Matter* . Vol. 64, p. 189.

Birnkman, A., Veldhuis, D., Mijatovic, D., Rijnders, G., Blank, D. H. A., Hilgenkamp, H.,Rogalla, H., 2001. "Superconducting quantum interfernce device based on MgB_2 nanobridges", *Applied Phys. Letters.* Vol. 79, p. 2420

Bouquet, F., Fisher, R. A., Phillips, N. E., Hinks, D. G., Jorgensen, J. D., 2001. "Specific heat of $Mg^{11}B_2$: evidence for a second energy gap", *Physical Review Letters*. Vol. 87, No. 25, p. 47001

Bu, S.D., Kim, D.M., Choi, J.H., Giencke, J., Hellstrom, E.E., Larbalestier, D.C., Patnik, S., Cooley, L., Eom, C.B., Lettieri, J., Scholm, D.G., Tian, W. and Pan, X.Q., 2002. "Synthesis and properties of c-axis oriented epitaxial MgB_2 thin films", *Appl. Phys. Letters.* Volume 81, No. 10, p. 1851.

Bud`ko, S. L., Lapertot, G., Petrovic, C., Cunningham, C. E., Anderson, N., Canfield, P.C. 2001. "Boron isotope effect in superconducting MgB_2**",** *Physical Review Letters*. Vol. 86, No. 9, p. 1877.

Buzea, C., Yamashita, T. 2001. "Review of the superconducting properties of MgB_2," *Superconductor Science and Technology*. Vol. 14 p. 115.

Chen, K., Ma, P., Nie, R.J., Yang, T., Xie, F.X., Liu, L.Y., Wang, S.Z., Dai, Y.D., Wang, F. 2002."Growth and superconductivity characteristics of MgB_2 thin films**",** *Superconductor Science and Technology*. Vol. 15**,** p. 1721.

Campel, S.A., 2001, "*The science and engineering of microelectronic fabrication"*, (Oxford University Press, New York), p. 249-251

Egilmez, M., Gunel, A., Okur, S., Tanoglu, M., Özyüzer, L. 2004. "Electrical and mechanical properties of MgB_2/Mg metal matrix composites", *Superconductor Science and Technology*. Vol. 19**,** p. 359.

Ermolov, S.N., Indenbom, M.V., Rossolenko, A.N., Bdikin, I.K., Uspenskaya, L.S., Stpeakov, N.S., Glebosvki, V.G. 2001, "Superconducting MgB_2 films obtained by magnetron sputtering", *JETP letters.* Vol. 73, No. 10, p. 626.

Erven, A.J.M., Kim, T.H., Muenzenberg, M., Moodera, J.S. 2002. "Highly crystallized as-grown smooth and superconducting MgB_2 films by molecular-beam epitaxy", A*pplied Physics Letters*. Vol. 81, No. 26, p. 4982.

Fan, Z.Y., Hinks, D.G., Newman, N., Rowell, J.M., 2001. "Experimental study of MgB_2 decomposition", *Applied Physics Letters.* Vol. 79, No. 1, p. 87.

Gavaler, J. R., Janocko, M. A., Jones, C. R. 1974. "Preparation and properties of high-T_c Nb-Ge films", *Journal of Applied Physics*. Vol .45, p. 3009.

Harada, Y., Uduka, M., Nakanishi, Y., Yoshimoto, N., Yoshizawa, M., 2004. "Synthesis of as-grown superconducting MgB_2 thin films by molecular beam epitaxy in UHV conditions", *Physica C: Superconductivity.* Vol. 412- 414, p. 1383.

He, T. Cava, R.J., Rowell, J.M., 2002. "Reactivity of MgB_2 with common substrate and electronic materials", *Applied Physics Letters.* Vol. 80, No. 2, p. 291.

Hinks, D.G., Claus, H., Jorgenson, J.D., 2001. "The complex nature of superconductivity in MgB_2 as revealed by the reduced total isotope effect", *Nature*. Vol. 411, p. 457.

Iavarone, M., Karapetrov, A., Koshelev, A.E., Kwok, W.K., Crabtree K.W., Hinks, D.G., Kang, W.N., Choi, E.M., Kim, H.J., Lee, S.I., 2002. "Two band gap superconductivity in MgB_2", *Physical Review Letters*. Vol. 89, No. 18, p. 187002.

Ionescu, M., McKinnon, J., Cai, C., Li, A., Konstantinov, K., Pan, A.V., Dou, S.X. 2002. "Growths of MgB_2 thin films by pulsed laser deposition", *Crystal Engineering.* Vol. 5, p. 391.

Jo, W., Huh, J.U., Ohnishi, T., Marshall, A.F., Beasly, M.R. and Hammond, R.H. 2002. " In situ growth of superconducting MgB_2 thin films with preferential orientation by moleculer-beam epitaxy", *Applied Physics Letters*. Vol. 80, No. 19, p. 3563.

Jung, M. H., Jaime, M., Lacerda, A.H., Boebinger, G.S., Kang, W. N., Kim, H.J., Choi, E.M., Lee, S.I. 2001. "Anisotropic superconductivity in epitaxial MgB_2 films", *Chemical Physics Letters.* Vol. 343, p. 447.

Kim, K. H. P., Choi, J. H., Jung, C. U., Chowdhury, P., Lee, H. S., Park, M. S., Kim, H. J., Kim, J. Y., Du, Zhonglian., Choi, E. M., Kim, M. S., Kang, W. N., Lee, S. I. 2002. "Superconducting properties of well-shaped MgB_2 single crystals", *Physical Review B.* Vol. 65, p. 100510.

Kim, H. J., Kang, W. N., Choi, E. M., Kim, M. S., Kim, K. H. P., Lee, S. 2001. " High current carrying capability in c-axis oriented superconducting MgB_2 thin films", *Physical Review Letters*. Vol. 87, No. 8, p. 08700.

Larbalestier, D., Gurevich, A., Feldmann, D. M., Polyanskii, A. 2001. "High-Tc superconducting materials for electric power applications", *Nature.* Vol. 414, p. 368.

Lee, S.G., Ahn, J.R., Kim, Y., Moon, S.H., Lee, K. W., Kim, I.S., Park, Y. K. 2003. "Properties of MgB_2 thin films made by radio frequency magnetron co-sputtering**",** *Superconductor Science and Technology*. Vol.16, p. 1550.

Liu, Z-k., Scholm, D. G., Li, Q., Xi, X. X. 2001. "Thermodynamics of the Mg–B system: Implications for the deposition of MgB_2 thin films**",** *Applied Physics Letters*. Vol. 78, No. 23, p. 3678.

Mancini, A., Galluzzi., V., Vetrella, U.B., Boffa, V., Celentano, G., Ciontea, L., Gambardella, U., Grassano, G., Petrisor, T., Rufoloni, A., Sprio, S., Vadrucci, M., "Properties of MgB_2 films grown by means of different vapor phase techniques", *IEEE Transactions on Applied Superconductivity.* Vol. 13, No. 2, p. 3305.

Meissner, W. and Ochsenfeld, R., 1933. "Ein neuer effect bei eintritt der supraleitfahigkeit", *Naturwissenchaften*, Vol. 21, No. 44, p. 787

Mijatovic, D., Birnkman, A., Veldhuis, D., Hilgenkamp, H., Rogalla, H., Rijnders, G., Blank, D.H.A., Pogrebnyakov, A.V., Redwing, J.M., Xu, S.Y., Li, Q., Xi, X.X. 2005. "SQUID magnetometer operating at 37 K based on nanobridges in epitaxial MgB_2 thin films", *Applied Physics Letters.* Vol. 87, p. 192505.

Moeckly, B.H. and Ruby, W.S. 2006. "Growth of high-quality large-area MgB_2 thin films by reactive evaporation", *Superconductor Science and Technology*. Vol. 19, p.21.

Moon, S.H., Yun, J.H., Lee H.N., Kye, J.I., Kim, H.G., Chung W., Oh B., 2001. "High critical current densities in superconducting MgB_2 thin films", *Appllied Physics Letters*. Vol. 79, No. 15, p. 2429.

Monticone, E., Gandini, C., Portesi, C., Rajteri, M., Bodoardo, S., Penazzi, N., Dellarocca, V., Gonelli, R.S., 2004. "MgB_2 thin films on silicon nitride subtrates prepared by an in situ method", *Superconductor Science and Technology*. Vol. 17, p. 649.

Mori, Z., Doi, T., Ishizaki, Y., Kitaguchi, H., Okada, M., Saitoh, K., Hakuraku, Y. 2004. "Superconducting properties of two-step in situ annealed MgB_2 thin films", *Physica C.* Vol. 412-414, p. 1371.

Nagamatsu, J., Nakagawa N., Muranaka, T., Zenitani, Y., Akimitsu, J. 2001. "Superconductivity at 39 K in magnesium diboride", *Nature.* Vol. 410, p. 63.

Naito, M., Ueada, K. 2004. "MgB_2 thin films for superconducting electronics", *Superconductor Science and Technology*. Vol. 17, p. 1.

Ohkuba, H., Akinaga, M., 2004. "Fabrication of as-grown superconducting MgB_2 thin films", *Physica C*. Vol. 408-410, p. 898.

Ohring, M., 2002. "*Material science of thin films"*, (Academic Press, San Diego), p. 358-359.

Osborn, R., Goremychkin, E. A., Kolesnikov, A. I., Hinks, D. G. 2001. "Phonon density of states in MgB_2", *Physical Review Letters*. Vol. 87, No. 1, p. 17005.

Onnes, H.K., 1911. "The disappearance of the resistivity of mercury", *Common. Leiden.* Vol. 122.b.

Patnaik, S., Cooley, L. D., Gurveich, A., Polyanski, A. A., Jiang, J., Cai, X. Y., Naus, M. T., Squiteri, A. A. A., Lee, M.K, Choi, J.H., Belenky, L., Bu, S. D., Letteri J., Song, X., Scholm, Babcock, D. S. E., Eom, C. B., Hellstrom, E. E., Larbalestier, D.C. 2001. "Electronic anisotropy, magnetic field-temperature phase diagram and their dependence on resistivity in *c*-axis oriented MgB_2 thin films", *Superconductor Science and Technology*. Vol. 14, p. 315.

Pogrebnyakov, A.V., Redwing, J.M., Jones, J.E., Xi, X.X., Xu, S.Y., Li, Q., Vaithyanathan, V., Schlom, D.G. 2003. "Thickness dependence of the properties of epitaxial MgB_2 thin films grown by hybrid physical-chemical vapor deposition", *Applied Physics Letters*. Vol. 82, No. 24, p. 4319.

Rowell, J. M. 2003."The widely variable resistivity of MgB_2 samples", *Superconductor Science and Technology*. Vol. 16, p. 17.

Schmidt, H., Zasadzinski, J.F., Gray, K.E., Hinks, D.G. 2002. "Evidence for two band-superconductivity from break-junction tunneling on MgB_2", *Physical Review Letters.* Vol. 88, No. 12, p. 127002

Shinde, S.R., Ogale, S.B., Greene, R.L., Venkatesan, T., Canfield, P.C., Bud'ko, S.L., Petrovic, C. 2001. "Superconducting MgB_2 thin films by pulsed laser deposition", Applied *Physics Letters*. Vol. 79, No. 2, p. 227

Ueda, K. and Naito, M. 2001. "As-grown superconducting MgB_2 thin films prepared by molecular beam epitaxy", A*pplied Physics Letters*. Vol. 79, No. 13, p. 2046.

Vaglio, R., Maglione, M.G., Capua, R. D. 2002. "High-quality MgB_2 thin films *in situ* grown by dc magnetron sputtering", *Superconductor Science and Technology*. Vol. 15, p. 1236.

Wördenweber R., 1999. "Growth of high-Tc thin films", *Superconductor Science and Technology*. Vol. 12, p. 86.

Wu, L.Y., Chang, C.N., Hsieh, C., Huang, B.J., Yang, H.C., Chen, J.M. 2004, "Study of the sputtered MgB_2 film on Al_2O_3 by x-ray absorption spectroscopy", *Chinese Jornal of Physics*. Vol. 42, No. 4-II, p. 534.

Xu, M., Kitazawa, H., Takano, Y., Ye, J., Nishida, K., Abe, H., Matsushita, A., Tsujii, N., Kido, G. 2001. "Anisotropy of superconductivity from MgB_2 single crystals", *Applied Physics Letters*. Vol. 79, No. 17, p. 2779.

Yang, D., Sun, H., Lu, H., Guo, Y., Li, X., Hu, X., 2003. "Experimental study on the oxidation of MgB_2 in air at high temperature", *Superconductor Science and Technology*. Vol. 16, p. 576.

Yildirim, T., Gulseren, O., Lynn, J. W., Brown, C. M., Oldovic T. J., Huang Q., Rogado N., Regan, K. A., Hayward, M. A., Slusky, J. S., He, T., Haas, M. K., Khalifah, P., Inummaru, K., Cava, P. C. 2001. "Giant anharmonicity and nonlinear electron-phonon coupling in MgB_2: a combined first-principles calculation and neutron scattering study", *Physical Review Letters.* Vol. 87, No. 3, p. 37001.

Zeng, X.H., Sukiasyan, A., Xi, X.X., Hu, Y. F., Wertz, E., Tian, W., Sun, H.P., Pan, X.Q., Lettieri, J., Scholm, D.G., Brubake, C.O., Lui, Z.K., Li, Q. 2001. "Superconducting properties of nanocrystalline MgB_2 thin films made by an in situ annealing process", *Applied Physics Letters*. Vol. 79, No. 12, p. 1840.

Zeng X., Pogrebnyakov, A. V., Kotcharov, A., Jones, J. E., Xi, X. X., Lyczek, E. M., Redwing, J. M., Xu, S., Li, Q., Letteieri, J., Schlom, D. G., Tian, W., Pan, X., Liu, Z. 2002. "In situ epitaxial MgB_2 thin films for superconducting electronics", *Nature Materials.* Vol. 1, p. 1.

Zeng, X., Pogrebnyakov, A.V., Zhu, M.H., Jones, J.E., Xi, X.X., Xu, S.Y., Wertz, E., Li, Q., Redwing, J.M., Lettieri, J., Vaithyanathan, V., Schlom, D.G., Liu, Z.K., Trithaveesak, O., Schubert, J. 2003. "Superconducting MgB_2 thin films on silicon carbide substrates by hybrid physical-chemical vapor deposition", *Applied Physics Letters*. Vol. 82, No. 13, p. 2097.

Zhang, Y.B., Zhu, H.M., Zhou, S.P., Ding, S.Y., Lin, Z.W., Zhu, J.G. 2006. "Uniform MgB_2 thin films grown on Si (111) and Al_2O_3 (0001) substrates prepared by e-beam evaporation and in situ annealing methods", *Journal of Applied Physics.* Vol. 99, p. 08M512.